PB92-137868

NOAA Technical Report, NWS 45

Functional Precision of National Weather Service Upper-Air Measurements Using VIZ Manufacturing Co. "B" Radiosonde (Model 1492-520)

Silver Spring, Md.
October 1991

U.S. DEPARTMENT OF COMMERCE
National Oceanic and Atmospheric Administration
National Weather Service

NOAA TECHNICAL REPORTS
National Weather Service Series

The National Weather Service (NWS) observes and measures atmospheric phenomena; develops and distributes forecasts of weather conditions and warnings of adverse weather; collects and disseminates weather informtion to meet the needs of the public and specialized users. The NWS develops the national meteorological service system and improves procedures, techniques, and dissemination for weather and hydrologic measurements, and forecasts.

NWS series of NOAA Technical Reports is a continuation of the former series, ESSA Technical Report Weather Bureau (WB).

Reports listed below are available from the National Technical Information Service, U.S. Department of Commerce, Sills Bldg., 5285 Port Royal Road, Springfield, VA 22161. Prices vary. Order by accession number (given in parentheses).

ESSA Technical Reports

WB 1 Monthly Mean 100-, 50-, 30-, and 10-Millibar Charts January 1964 through December 1965 of the IQSY Period. Staff, Upper Air Branch, National Meteorological Center, February 1967, 7 p, 96 charts. (AD 651 101)

WB 2 Weekly Synoptic Analyses, 5-, 2-, and 0.4-Mb Surfaces for 1964 (based on observations of the Meteorological Rocket Network during the IQSY). Staff, Upper Air Branch, National Meteorological Center, April 1967, 16 p, 160 charts. (AD 652 696)

WB 3 Weekly Synoptic Analyses, 5-, 2-, and 0.4-Mb Surfaces for 1965 (based on observations of the Meteorological Rocket Network during the IQSY). Staff, Upper Air Branch, National Meteorological Center, August 1967, 173 p. (AD 662 053)

WB 4 The March-May 1965 Floods in the Upper Mississippi, Missouri, and Red River of the North Basins. J. L. H. Paulhus and E. R. Nelson, Office of Hydrology, August 1967, 100 p.

WB 5 Climatological Probabilities of Precipitation for the Conterminous United States. Donald L. Jorgenson, Techniques Development Laboratory, December 1967, 60 p.

WB 6 Climatology of Atlantic Tropical Storms and Hurricanes. M. A. Alaka, Techniques Development Laboratory, May 1968, 18 p.

WB 7 Frequency and Areal Distributions of Tropical Storm Rainfall in the United States Coastal Region on the Gulf of Mexico. Hugo V. Goodyear, Office of Hydrology, July 19968, 33 p.

WB 8 Critical Fire Weather Patterns in the Conterminous United States. Mark J. Schroeder, Weather Bureau, January 1969, 31 p.

WB 9 Weekly Synoptic Analyses, 5-, 2-, and 0.4-Mb Surfaces for 1966 (based on meteorological rocket-sonde and high-level rawinsonde observations). Staff, Upper Air Branch, National Meteorological Center, January 1969, 169 p.

WB 10 Hemispheric Teleconnections of Mean Circulation Anomalies at 700 Millibars. James F. O'Connor, National Meteorological Center, February 1969, 103 p.

WB 11 Monthly Mean 100-, 50-, 30-, and 10-Millibar Charts and Standard Deviation Maps, 1966-1967. Staff, Upper Air Branch, National Meteorological Center, April 1969, 124 p.

WB 12 Weekly Synoptic Analyses, 5-, 2-, and 0.4-Millibar Surfaces for 1967. Staff, Upper Air Branch, National Meteorological Center, January 1970, 169 p.

NOAA Technical Reports

NWS 13 The March-April 1969 Snowmelt Floods in the Red River of the North, Upper Mississippi, and Missouri Basins. Joseph L. H. Paulhus, Office of Hydrology, October 1970, 92 p.

NWS 14 Weekly Synoptic Analyses, 5-, 2-, and 0.4-Millibar Surfaces for 1968. Staff, Upper Air Branch, National Meteorological Center, May 1971, 169 p. (COM-71-50383)

NWS 15 Some Climatological Characteristics of Hurricanes and Tropical Storms, Gulf and East Coasts of the United States. Francis P. Ho, Richard W. Schwerdt, and Hugo V. Goodyear, May 1975, 87 p. (COM-75-11088)

NWS 16 Storm Tide Frequencies on the South Carolina Coast. Vance A. Myers, June 1975, 79 p. (COM-75-11335)

NWS 17 Estimation of Hurricane Storm Surge in Apalachicola Bay, Florida. James E. Overland, June 1975. 66 p. (COM-75-111332)

(Continued on last page)

BIBLIOGRAPHIC INFORMATION

PB92-137868

Report Nos: NOAA-TR-NWS-45

Title: Functional Precision of National Weather Service Upper-Air Measurements Using VIZ Manufacturing Co. 'B' Radiosonde (Model 1492-52Ø).

Date: Oct 91

Authors: P. Ahnert, M. Gelman, and M. Lukes.

Performing Organization: National Weather Service, Silver Spring, MD.**National Meteorological Center, Washington, DC.

Type of Report and Period Covered: Technical rept.

Supplementary Notes: See also PB92-137843 and PB92-13785Ø. Prepared in cooperation with National Meteorological Center, Washington, DC.

NTIS Field/Group Codes: 55D, 55C

Price: PC AØ3/MF AØ1

Availability: Available from the National Technical Information Service, Springfield, VA. 22161

Number of Pages: 46p

Keywords: *Meteorological instruments, *Radiosondes, Balloon-borne instruments, Acceptance tests, Atmospheric temperature, Barometric pressure, Temperature measurement, Humidity measurement, Troposphere, Stratosphere, Precision, Comparison.

Abstract: The functional precision of VIZ Model 1492-52Ø (VIZB) radiosonde was determined using the National Weather Service functional analysis test package. The comparisons were made from 33 flights of paired radiosondes suspended from the same balloon. Functional precision is given by the root mean square of the differences between measurements made by 2 sensors of the same type exposed to the same environment. Results are summarized for simultaneous measurements at one minute intervals as well as measurements at a predefined set of pressure levels. These tests were conducted for the acceptance of contract production samples and results are reported here for use by the meteorological community in specifying the characteristics of this radiosonde, which operational use started in 1989.

PB92-137868

NOAA Technical Report, NWS 45

Functional Precision of National Weather Service Upper-Air Measurements Using VIZ Manufacturing Co. "B" Radiosonde (Model 1492-520)

Office of Systems Operations
Engineering Division
Test and Evaluation Branch
Sterling, Va.
October 1991

U.S. DEPARTMENT OF COMMERCE
Robert A. Mosbacher, Sr.; Secretary

National Oceanic and Atmospheric Administration
William E. Evans; Under Secretary

National Weather Service
Elbert W. Friday, Jr.; Assistant Administrator

ACKNOWLEDGEMENTS

Test report creation is credited to Peter Ahnert, currently at the NWS Weather Service Office in Harrisburg, PA. Extensive critical review and contributions are credited to Mel Gelman at the National Meteorological Center, Climate Analysis Center in Camp springs, MD. Revision to final draft and publication arrangements are credited to Mike Lukes of the NWS Test and Evaluation Branch at Sterling Research and Development Center, Sterling, VA.

Radiosonde flights and data processing were performed by the Test Branch of T&EB. Special thanks to Jim Fitzgibbon, Gene Hollingsworth, Dick Bollinger and Mike Ross for their long hours and dedication resulting in high quality data. Excellent maintenance support was provided by Dean Carson, of the T&EB Support Branch. Many others at T&EB also made contributions. The integrated functional test software, which made the detailed analysis of the data possible, was developed by Peter Hammett of the Network Software Branch, Office of System Operations (OSO). Thanks also to thank Joe Facundo of the Observing Systems Branch, OSO for his support and assistance.

TABLE OF CONTENTS

LIST OF FIGURES

LIST OF TABLES

ABSTRACT

FUNCTIONAL PRECISION OF NATIONAL WEATHER SERVICE
UPPER-AIR MEASUREMENTS USING
VIZ MANUFACTURING CO. "B" RADIOSONDE (MODEL 1492-520)

Test and Evaluation Branch, National Weather Service, NOAA
Sterling, Va.

The functional precision of VIZ Model 1492-520 (VIZB) radiosonde was determined using the National Weather Service functional analysis test package. The comparisons were made from 33 flights of paired radiosondes suspended from the same balloon. Functional precision is given by the root mean square of the differences between measurements made by 2 sensors of the same type exposed to the same environment. Results are summarized for simultaneous measurements at one minute intervals as well as measurements at a predefined set of pressure levels. These tests were conducted for the acceptance of contract production samples and results are reported here for use by the meteorological community in specifying the characteristics of this radiosonde, which operational use started in 1989.

For comparisons made at one minute intervals, the overall functional precision for temperature was 0.3°C and ranged from 0.3°C to 0.4°C. The precision for pressure ranged from 1.6 mb to 2.6 mb in the troposphere below 100 mb, and 1.1 mb to 1.8 mb in the stratosphere, with an overall value of 2.0 mb. Relative humidity precision was less than 2 percent.

For comparisons made at predefined pressure levels, the functional precision for height ranged from about 2 meters near 850 mb to 21 meters near 100 mb. The precision for temperature ranged from 0.4°C to 0.6°C in the troposphere to 0.5°C to 1.0°C in the stratosphere. Relative humidity precisions were less than 3 percent.

Compared to the VIZA (Model 1492-510) time-commutated sonde, precisions for data sampled at the same time for relative humidity and dew-point were better (smaller RMSD) remained about the same for temperature, and became worse (larger RMSD) for pressure. Both tests used the same automated data recording and reduction methods. Differences are mainly attributed to the radiosonde design modifications and sensor placement.

1. BACKGROUND

Functional Testing is a procedure which determines bias and variability between data sets of meteorological measurements made by two separate instruments or observation systems which are exposed to the same environment at the same time. If the data sets are provided by identical systems, the root mean square of the differences (RMSD) is a measure of variability and is termed the Functional Precision. If they are provided by dissimilar systems, the RMSD is termed Functional Comparability and the mean of the differences is the bias. For upper-air testing, the data can be compared not only at the same time but also at the same pressure. The terms and testing procedures were developed by Walt Hoehne in 1971 and functional tests on the operational NWS radiosondes were performed in 1973 and 1979 (Hoehne, 1971, 1980).

The National Weather Service (NWS) has been flying radiosondes made by VIZ Manufacturing Co. (formerly Molded Insulation Co.) since 1958. The VIZ Model 1492-510 (VIZA) was used in the NWS synoptic upper-air network from 1986 until 1989. In 1988, the VIZA production contract expired and the NWS awarded contracts to VIZ Manufacturing Co. and the Space Data Corporation (currently Space Data Division of Orbital Sciences Corp.). VIZ was to produce the redesigned Model 1492-520 (VIZB) radiosondes for synoptic soundings at 60-65 of the U.S. upper-air stations and Space Data for 15-20 U.S. stations.

The advantage of introducing another, independent source for radiosondes is to insure an adequate supply to continue operations if a manufacturer's production capability is lost or diminished. Also, increased competition among vendors theoretically improves cost, efficiency and product quality. A major disadvantage of a multi-sonde network is that it produces an inhomogeneous synoptic data set which, when used for model initialization, can severely degrade analyses and forecasts. Modeling techniques cannot totally compensate for this type of data anomaly. Also, changes in the radiosonde sensors and their characteristics limit the usefulness of radiosonde data for long term climatological studies. Other disadvantages include a significant increase in the test and evaluation requirements. It is necessary to determine the functional precision of a radiosonde and its comparability to any other radiosonde in concurrent or previous use.

Early in 1988, The NWS Test and Evaluation Branch, within the Engineering Division of the Office of Systems Operations, initiated tests in support of the new radiosonde procurement. Both radiosondes were designed according to functional specifications which gave the manufacturer maximum flexibility towards meeting performance requirements. Formal acceptance of the VIZB and Space Data sondes followed successful performance testing. The VIZA sonde was phased out by February, 1989, by which time all conterminous U.S. and Alaskan stations had switched to either the VIZB or the Space Data sonde.

The VIZB sonde is similar to the VIZA sonde. The radiosonde case, meteorological data oscillator (MDO), and transmitter circuitry were redesigned and, although the pressure, temperature, and humidity sensors remained unchanged, their orientation, mounting and exposure changed with the new design.

Functional precision testing of the VIZA and Space Data sonde, and functional comparability testing of the VIZA to the VIZB and Space Data sondes are described in separate test reports. A paper summarizing all test results was presented at the Upper-Air Measurements and Instrumentation Workshop, November 14-16, 1989, at Wallops Island, VA and at the American Meteorological Society's Seventh Symposium on Meteorological Observations and Instrumentation, January 14-18, 1991, at New Orleans, LA (Ahnert, 1991). A few differences may exist between the test results reported herein and those in the paper due to subsequent data editing for better quality control and statistical accuracy.

2. INSTRUMENT DESCRIPTION

The VIZB (Model 1492-520) radiosonde is an expendable instrument package that is suspended below an ascending balloon. The radiosonde measures the vertical profiles of pressure (P), temperature (T), and relative humidity (U) of the atmosphere as it ascends. These meteorological parameters are measured by sensors and the measurements are transmitted to the ground by radio. The VIZB radiosonde (Figure A1) consists of sensors, telemetry electronics, radio transmitter, and wet-cell battery enclosed in a styrofoam case. The radiosonde physical dimensions are 6.5 X 5 X 12 inches and weighs 640 gm with activated battery.

The VIZ radiosonde transmits meteorological data to the ground receiving equipment using a 1680 MHz carrier wave which has been amplitude modulated into a pulse-train. The met data information is contained in the pulse repetition frequency, which may range from 100 Hz to 1 KHz and varies with the value of the parameter being measured. Each quarter second, the transmitted pulse-train is sequentially switched (time-commutated) between P, T, U, and the internal reference. This produces a cyclic pulse-train which represents a nominal one second sampling rate of the meteorological parameters by the radiosonde.

The pulse-train repetition frequency is controlled by sensor resistance, which varies the output of an audio frequency oscillator, referred to as the Met Data Oscillator (MDO). The sensor resistance is a function of the meteorological parameter being measured. A high resistance causes the MDO to oscillate at a low frequency and visa-versa. The pulse repetition frequencies from sensors for pressure, temperature, and relative humidity and an internal reference are time-commutated in the MDO circuit. (Systex, 1990).

The VIZB pressure sensor is the same used in the VIZA radiosonde. It is a baroswitch which consists of an aneroid pressure cell (evacuated diaphragm) which expands or contracts in response to pressure changes. This expansion/contraction is mechanically linked to a pen arm which moves (in a vertical plane) across a set of discrete contacts. Each contact corresponds to a particular pressure. Whenever the pen arm moves from one contact to another, a step change in resistance results in a corresponding step change in telemetered pulse repetition frequency for pressure. On the ground, the telemetered pressure signal is converted to a pressure value by using the baroswitch's calibration data. Each baroswitch is individually calibrated by the manufacturer. The pressure sensor is located inside the top part of the styrofoam case, along with the Met Data Oscillator (MDO) board. The baroswitch is mounted in a differently than that of the VIZA, resulting in a vertically oriented pen-arm rather than horizontal.

The temperature sensor is the same thermistor used in the VIZA radiosonde. It is a rod about 2 inches long and a diameter of no more than 0.05 inches, when coated. It is a negative resistance thermistor composed of a baked mixture of clay and iron filings. It is coated with white, lead carbonate paint in order to reduce the solar radiation effects and to standardize its solar response across production lots. At high altitudes, the white coating does not strongly reduce the infrared influence of the atmosphere. This can cause nighttime temperature errors in excess of 1.5°C when the sonde is above 10 mb (Schmidlin, Luers, and Huffman, 1986). Each lot of thermistors is made from one batch of the iron and clay mixture. For a given mixture, the thermistors will follow a characteristic temperature-resistance curve family. Each thermistor is calibrated by measuring its resistance at two temperatures to determine the lock-in value for its specific curve. In order to mitigate thermal influences from the radiosonde case, the thermistor is mounted on coated wire leads on the end of a stiff but flexible insulated wire which extends 6.5 inches from the radiosonde and angled to a position about 1 inch above the top of the case. This differs from the VIZA which had the thermistor attached to a plastic frame extending from the radiosonde.

The humidity sensor is the same carbon element hygristor used in the VIZA radiosonde. It consists of a strip of plastic (2.5 X 0.7 X 0.03 inches) which has been dipped in a mixture of carbon particles dispersed in a celluloid resin and then dried. When an electric current is passed through the carbon-celluloid coating, it acts as a resistor. The celluloid is sensitive to relative humidity and expands or contracts with the amount of water vapor available. This causes a greater average distance between carbon particles and thus increases its resistance. As with temperature, each sensor for a particular lot follows a characteristic relative humidity-resistance curve family. Each hygristor is then cycled through increasing and decreasing humidity, and then scribed to produce the correct resistance at the 33% lock-in value. Due to a change in the elastic properties of the sensor materials near -40°C, the NWS does not report humidities for temperatures below that. Also, the transfer equation that is used to convert resistance to humidity is suspect at the low end and relative humidities below 20% are not reported. To simplify humidity determinations, the transfer equation uses the temperature sensed by the outboard thermistor instead of the hygristor temperature. If a there is a temperature difference between the two, the calculated RH is in error. To reduce the temperature difference, the carbon hygristor, it is housed inside a "J" shaped duct within the top half of the styrofoam radiosonde case. The surface of the duct is coated with a black laminate intended to protect the hygristor from heating by reflected solar radiation. The hygristor in the VIZB duct seems to be better insulated from solar and sonde heating than for the VIZA sonde.

3. TEST METHODOLOGY

For this test, data from 33 dual radiosonde flights were used. Of these, 15 were daytime and 18 were nighttime releases. The dual flights consisted of two VIZB radiosondes suspended from one balloon. Early in the test, a few triple releases were made, which included a third sonde of another type. Triple flights were discontinued after problems with radio frequency interference and additional personnel requirements made them impractical. All flights for this test were made at the Sterling Research and Development Center, Sterling, VA located 20 miles west of Washington, D.C.

3.1 RADIOSONDE PREPARATION/RELEASE

A 600 gram or larger balloon was prepared and filled with hydrogen gas to a nozzle lift of 2500-3000 grams. The balloon train included 2 parachutes and terminated with a 6 foot styrofoam spreader bar. The radiosondes were hung 3 feet below each end of the horizontal spreader bar. The train length ranged from 120 feet for low wind speeds to 50 feet in strong winds.

Both VIZB sondes were prepared and released according to standard NWS operating procedures (NWS, 1981). The transmitters were adjusted so the frequency separation was at least 10 MHz.

Initial releases required at least one person at the release site and another person at the ground system console, located a half mile away. Through radio contact and visual confirmation, the release button at the console was pressed when the radiosondes became airborne. During the initial period of this test, two ART remote-control units were installed at the release site. This, combined with a radio triggered release switch, allowed for 1 person releases in low surface winds and 2 person releases otherwise.

3.2 GROUND EQUIPMENT

The ground equipment consisted of two ART systems and minicomputers, designated ART-1R and ART-2R. Both system configurations were identical to operational NWS equipment. The ART-1R uses a GMD type radiotheodolite and the ART-2R uses a WBRT type radiotheodolite. Most of the ART electronics are solid state. Differences between the systems occasionally result in discrepancies in signal strength and noise levels but these will not induce any biases in the pressure, temperature, and humidity data. Since wind data characteristics are primarily a function of the ground equipment and not the radiosonde, they were not analyzed as a part of this test.

3.3 DATA REDUCTION

The VIZB sonde uses a 1680 MHz carrier wave to cyclically transmit sensor data, as a pulse-train, at a nominal rate of once per second. The cycle's (i.e., data frame) sequence corresponds to the sensed pressure (P), temperature (T), relative humidity (U), and high or low reference values. The pulse-train for each parameter is transmitted for a quarter of the cycle and is referred to as the data sub-frame for that parameter. For each sub-frame, the sensor resistance, which corresponds to the parameters' value, determines a pulse repetition frequency between 100 and 1 KHz. During the sub-frame transmission, the MDO frequency modulates the amplitude of the carrier wave so that it is large for a period which corresponds to the correct pulse repetition frequency for the value of the met parameter. The radiosonde signal is then received and automatically tracked by the radiotheodolite's parabolic antenna. The ART receiver amplifies the subframe signal to 0.5 volts. The pulse-train signal is sent to the ART Interface Board (ARTIB) located in the minicomputer. For each sub-frame, the ARTIB measures the time of arrival for each pulse and interrupts the minicomputer.

Using the ARTIB generated interrupts, the minicomputer software synchronizes with the radiosonde commutation cycle, computes the average period values for reference and each data subframe, and stores the data. After synchronization, the data is filtered using a histogram technique. This separates the dominant frequency from the noise and assigns a data quality indicator for each subframe. From the sub-frame data, an average value for a six second interval is calculated for temperature, relative humidity, and reference frequencies. This produces a data set with an effective 0.1 minute sampling rate. Since the frequency of the pressure sub-frame will only change when the baroswitch pen-arm reaches a different contact, the computer monitors the sub-frame for these frequency shifts and determines which pressure contact it is on. The 6 second pressure values are interpolated between contacts. The frequency data form the data set stored on the minicomputer system tape.

Although the minicomputer continues on to select mandatory and significant levels and compose messages, that information was not used for these tests. Following each flight the 6 second frequency data were transferred from the system tape to a second log tape. Then the microcomputer was booted from a special system tape and a program run to dump the data from the log tape to a microcomputer at 2400 bps. The microcomputer then dumped the data to a floppy disk.

The data reduction was done on the microcomputer. Surface and radiosonde administrative data were entered. The microcomputer processed the 6 second frequency data into meteorological units of pressure (mb), temperature (C), relative humidity (%), and height (m). From this 6 second met data, one minute and mandatory level data were extracted, put into the "RAWIN.DAT" file, and written to floppy disk.

The one minute data were obtained by extracting the met data from the 6 second data period which contained the whole minute. If the met data value was missing for the 6 second data, it was also reported as missing for the one minute data (i.e., no interpolation was performed).

The mandatory level data were obtained from the 6 second frequency data by first determining, to the nearest 0.06 second, when the radiosonde reached the mandatory pressure. Then, temperature, humidity, and heights for that time were interpolated, using the 6 second frequency data which bracketed the mandatory level. If either of those 6 second values was missing, then the mandatory level value was also reported as missing.

The two floppy disks containing the RAWIN.DAT files for the two radiosondes flown were then clearly identified and catalogued. When time permitted, the dual flight data were loaded into the Functional Analyses Testing Package (FATP). This software package runs on a 80286 microcomputer and consists of off-the-shelf database, statistics, and graphics software. These have been integrated with customized software to perform functional analyses of dual radiosonde data. After entering the data from each flight, it was plotted and reviewed. All statistics, tables and figures contained herein were produced by the FATP.

4. COMPARISONS BY TIME

The time comparisons for pressure, temperature, relative humidity and dew-point depressions were made using the one minute data. One minute heights were extracted from 6 second calculated heights. If that height was missing, no interpolation was performed and the one minute height was reported as missing. Since the radiosondes were horizontally separated, they were essentially sampling the same environment at the same time. For each minute of the flight, the Functional Analyses Testing Package (FATP) computed differences of pressure, temperature, relative humidity, dew-point depression, and height between the two radiosondes and the difference statistics for the total population were computed. The root mean square of the differences (RMSD) was used to indicate the functional precision for that parameter, as measured by the particular radiosonde. Biases and skewness are artificial since the assignation of primary and secondary sonde is purely arbitrary. The kurtosis (flatness) for a normal distribution has a value of 3.0.

Histograms, frequency tables, scatter plots and linear regressions were also generated using the FATP software. Where possible the measurement range was divided into intervals and the functional precision for each interval was computed. This can provide insight on the variability of performance over the measurement range. For pressure, temperature, and relative humidity, precision was also computed for intervals of pressure corresponding to analyses done during the World Meteorological Organization (WMO) international radiosonde intercomparisons.

4.1 PRESSURE

For the total population, 83.0% of pressure differences by time were within ±2.0 mb, 55.2% were within ±1.0 mb, and 7.3% exceeded ±3.0 mb (Figure 1, Table 1). The relative frequencies for the magnitude of pressure difference occurring within a difference interval are given for 6 pressure layers (Table 1).

The scatter plot (Figure 2) shows a number of points from flight #169 where primary pressures exceeded secondary pressures by 8 to 10 mb. Figure A-2 shows the pressure difference for each minute of flight #169 and indicates that one or both radiosondes had large pressure errors.

The overall functional precision (RMSD) for pressure by time is 2.0 mb (Table 1). For the 6 pressure layers, precisions ranged from 1.3 mb for the layer above 20 mb to 2.3 mb for the layer between 100 and 500 mb. For all layers, the precision is worse (larger RMSD) than corresponding values for the VIZA sonde and is nearly double for the 50 to 100 mb layer (NWS, 1991). A table and graph with precisions for 12 pressure intervals used in the WMO intercomparisons are also included (Figure 3, Table 3).

The overall functional precision of the VIZB sonde for pressure compared by time is 0.7 mb worse than the VIZA sonde used by NWS from 1986-1989 (NWS, 1991). It is about the same as the VIZ pressure-commutated radiosonde tested in 1980 (Hoehne, 1980) and is equal to the functional precision required by the current radiosonde specification.

Although the large pressure differences of flight #169 have contributed to the degradation of the VIZB pressure precision compared that of the VIZA sonde, another possible contribution could be the pendular swinging of the balloon-radiosonde system which may induce extraneous movements of the baroswitch's pen-arm, which is vertically oriented in the VIZB sonde. Minor differences in manufacture and calibration quality may have also contributed to the degradation.

4.2 TEMPERATURE

For the total population, 94% of the temperature differences by time were ±0.5°C or less (Figure 4, Table 4). The relative frequencies for the magnitude of temperature difference occurring within a difference interval are given for 7 intervals (Table 4).

The scatter plot (Figure 5) shows increasing scatter at lower temperatures and some anomalous points belonging to flight #15, which was a short flight with temperature differences ranging from 1.0°C to 2.0°C (Figure 5, Figure A-3).

The overall functional precision (RMSD) for temperature by time is 0.31°C (Table 4). For the 7 temperature intervals, precisions varied slightly with temperature. It ranged from 0.25°C between -40 and -20°C to 0.39°C between +5 and +20°C. Precision becomes systematically better (smaller RMSD) as temperature decreases from +20 to -40°C and then worsens (RMSD increases) for temperatures below -40°C. The precision for the interval between +20 and +35°C is based on a small sample size of 55 and should be used with caution. Precisions for 12 pressure intervals used in the WMO intercomparisons are presented in Figure 6 and Table 6.

Overall functional precision of the VIZB radiosonde for temperature compared by time is 0.03°C better (smaller RMSD) than reported for the VIZA sonde (NWS,1991) and is well within the current functional precision requirement of 0.5°C.

4.3 HUMIDITY

Relative humidity is measured by the radiosonde hygristor in terms of electrical resistance. It is converted to dew-point depressions for message coding and transmission to other users. To determine a measure of humidity from the dew-point depression, the temperature must be known, so, if the temperatures reported by both sondes used in the comparisons are not the same, the dew-point depression differences do not give a pure measure of the humidity statistics but rather a combined measure of temperature and humidity statistics which are difficult to objectively analyze.

4.3.1 RELATIVE HUMIDITY

For the total population, 98.2% of the Relative Humidity differences by time were within ± 5.0% RH (Table 7). The relative frequencies for the magnitude of relative humidity difference occurring within a difference interval are given for 9 relative humidity ranges (Table 7).

The scatter plot (Figure 8) clearly indicates increased spread at lower humidities. The largest relative humidity difference wad 8.2% (Table 8).

The overall functional precision (RMSD) for relative humidity by time is 1.6% RH (Figure 7, Table 7). For the 9 relative humidity intervals, precisions ranged from 0.5% RH between 90 and 100% RH to 3.4% RH between 20 to 30% RH. Precisions for 5 pressure intervals used in the WMO intercomparisons are given in Figure 9 and Table 9. The data reveal a high degree of uniform degree of uniformity in precision (1.3% to 1.8% RH) over the pressure range. However, this does not mean that absolute accuracy of the carbon element hygristor remains unaffected by lower pressures or colder temperatures encountered at high altitudes.

The overall functional precision of the VIZB sonde for relative humidity compared by time is 0.5% better (lower RMSD) than for the VIZA sonde (NWS,1991). The current radiosonde specifications require the functional precision for relative humidity to be less than 5.0% RH.

The standard NWS 20% RH cutoff was not applied to these data since it would have caused considerable problems with the statistics. Please note, however, that the accuracies of humidities below 20% RH calculated using current NWS equations is questionable and indicated precisions at these humidities may not reflect a trend in precision for the measurement range.

4.3.2 DEW-POINT DEPRESSION

The overall functional precision (RMSD) for dew-point depression by time is 2.4°C (Table 10). This is 1.1°C better (smaller RMSD) than the precision for the VIZA sonde (NWS,1991) and 1.3°C better than the VIZ pressure commutated radiosonde (Hoehne, 1980).

Unfortunately, computed statistics in these and Hoehne's tests are affected by the NWS practice of assigning dew point depressions of 30°C whenever measured relative humidity is at or below 20% RH. This affects the statistics in the following two ways. First, when both sondes are measuring 20% RH or less, both get assigned depressions of 30°C, and a false number of cases indicating no differences are used in the statistics. Secondly, if one sonde measures slightly above 20% RH and the other measure 20% RH or less, an artificially large difference value is used in the statistics. The large differences are visible in the histogram of dew point depression differences (Figure 10). These two effects tend to cancel each other out to some extent but it is not known whether the net effect is to increase or decrease the estimated functional precision.

4.4 HEIGHT

The overall functional precision (RMSD) of height by time is 159 meters (Figure 11, Table 11). This is 56 meters worse (larger RMSD) than the precision for the VIZA sonde (NWS,1991). Note that height versus time data are rarely, if ever, used in meteorological analyses. Height measurements of pressure levels are discussed in section 5.3.

Comparing the magnitude of height differences with height produced a strong correlation of 0.51 (i.e., more height scatter at greater heights).

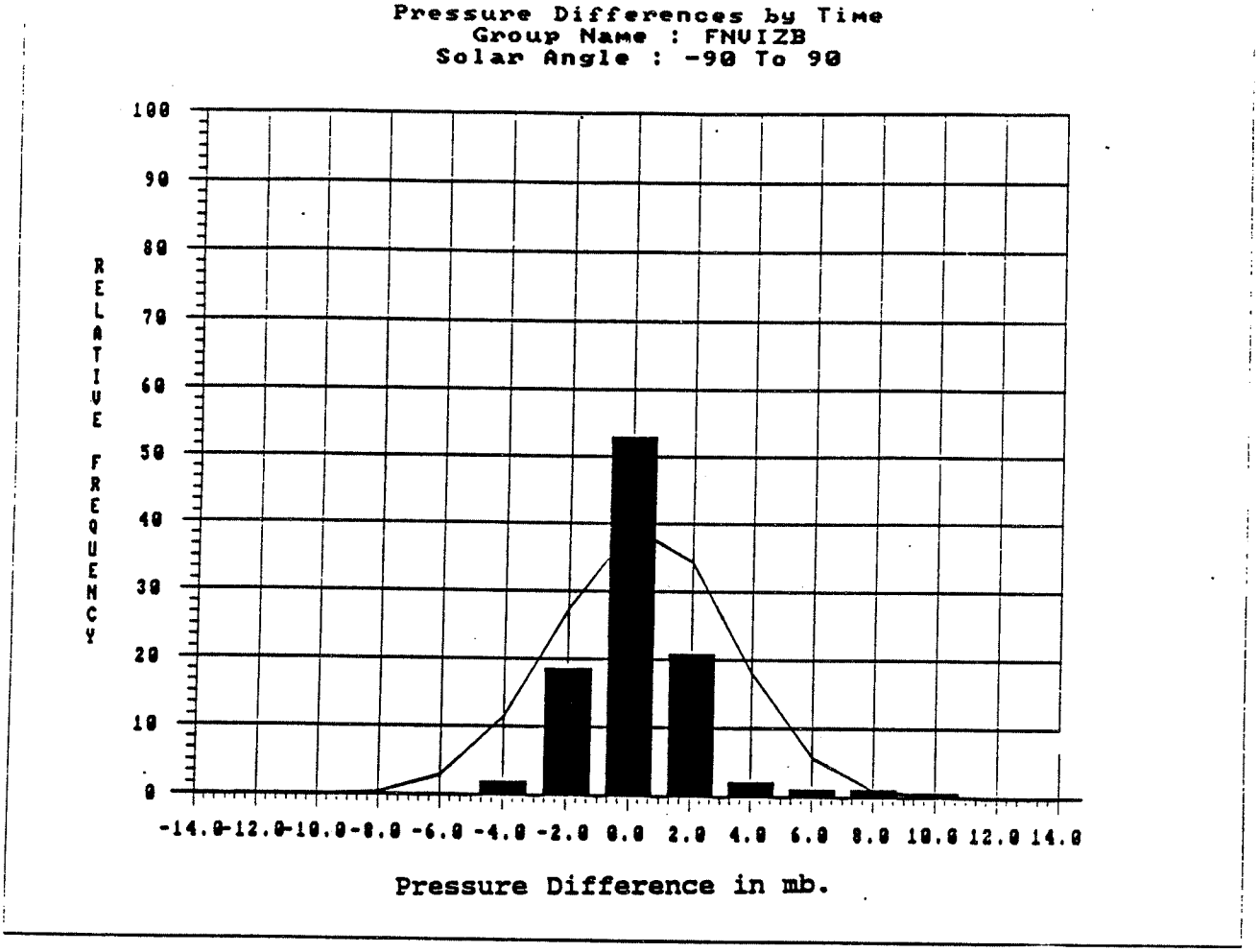

Figure 1. Histogram of Pressure Difference sampled at same time of flight Normal curve computed from sample mean and standard deviation.

MB. FROM		TO	SAMPLE SIZE	# OF FLIGHTS	Absolute Pressure Difference Interval 0.0-0.5	0.6-1.0	1.1-1.5	1.6-2.0	2.1-2.5	2.6-3.0	> = 3.1	MEAN DIFF.	RMS DIFF.	STD.DEV. DIFF.
					Relative Frequency in %									
850.0	THRU	1009.9	159	33	34.0	26.4	15.1	8.2	3.1	5.0	8.2	.18	1.58	1.57
500.0	THRU	849.9	503	33	26.4	21.9	19.3	8.9	5.8	5.8	11.9	.53	2.21	2.15
100.0	THRU	499.9	1159	33	25.5	24.0	15.4	13.8	8.6	4.8	7.9	.51	2.28	2.23
50.0	THRU	99.9	380	29	34.7	29.7	16.6	8.2	6.8	0.0	3.9	.38	1.70	1.66
20.0	THRU	49.9	358	25	34.9	36.6	11.7	13.1	.6	0.0	3.1	.26	1.50	1.48
0.0	THRU	19.9	56	12	30.4	19.6	16.1	33.9	0.0	0.0	0.0	.50	1.26	1.16
	ALL		2617	33	29.0	26.2	15.8	12.0	6.2	3.6	7.3	.44	2.04	1.99

Table 1. Frequency of occurrence (%) of Absolute Pressure Difference within selected pressure layers and for all data. Mean, rms (functional precision), and std. dev. of Pressure Difference for layers and all data. Sampled at same time of flight.

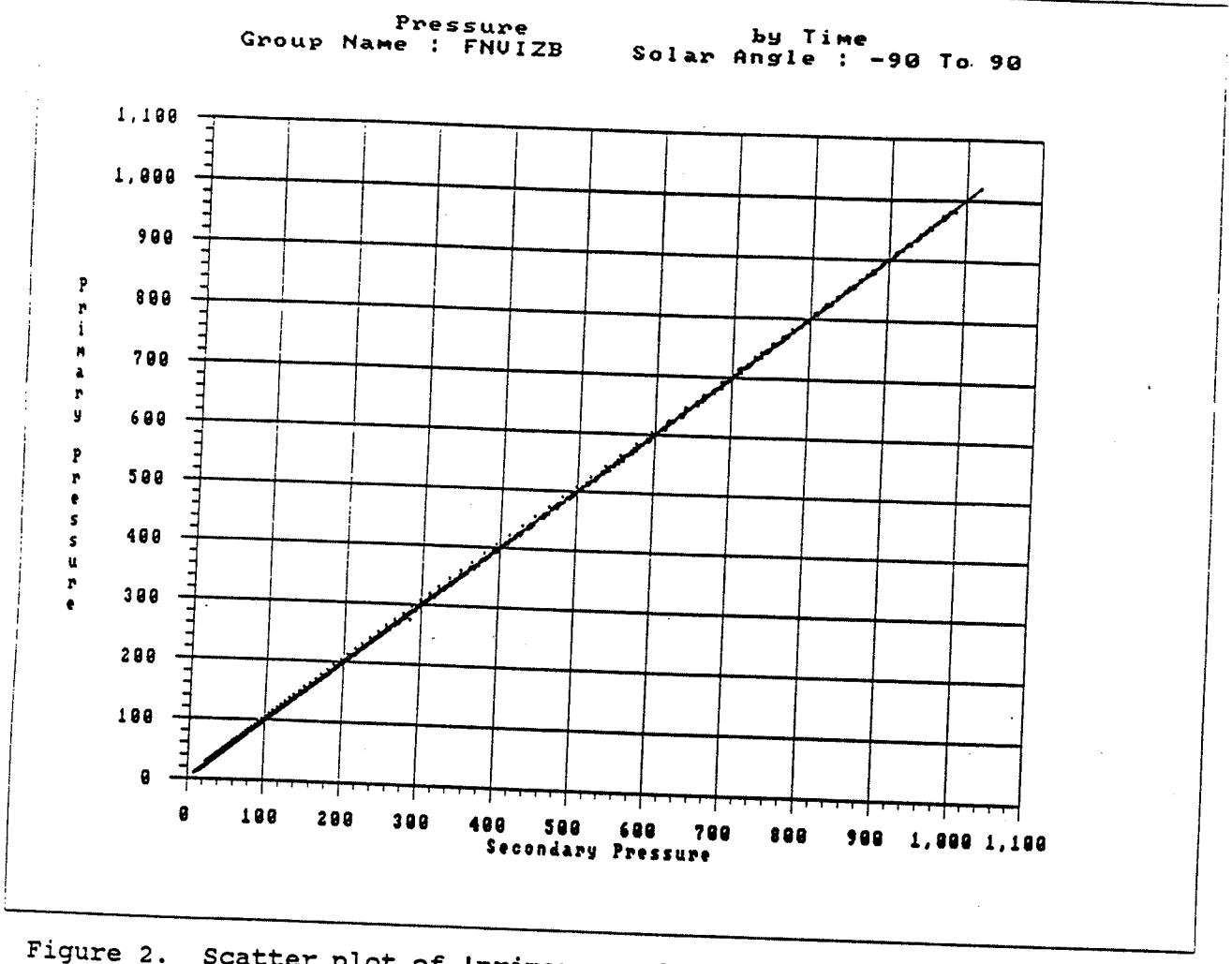

Figure 2. Scatter plot of 'primary sonde' Pressure versus 'secondary sonde' Pressure sampled at same time of flight. Regression line also plotted.

SAMPLE SIZE	# OF FLIGHTS	MEAN DIFF	STD DEV DIFF	RMS DIFF	SKEW. DIFF	KURT. DIFF	CORR. P & S	PRIM MIN	PRIM MAX	SECOND MIN	SECOND MAX	DIFFER MIN	DIFFER MAX
2617.0	33	.44	1.99	2.04	1.65	9.62	1.00	10.50	1020.00	9.10	1020.00	11.10	11.10

Table 2. Pressure sampled at same time of flight. Mean, std. dev., rms, skewness, and kurtosis of differences. 'Primary sonde' and 'secondary sonde' correlation. Minimum and maximum Pressure and Pressure Difference in mb.

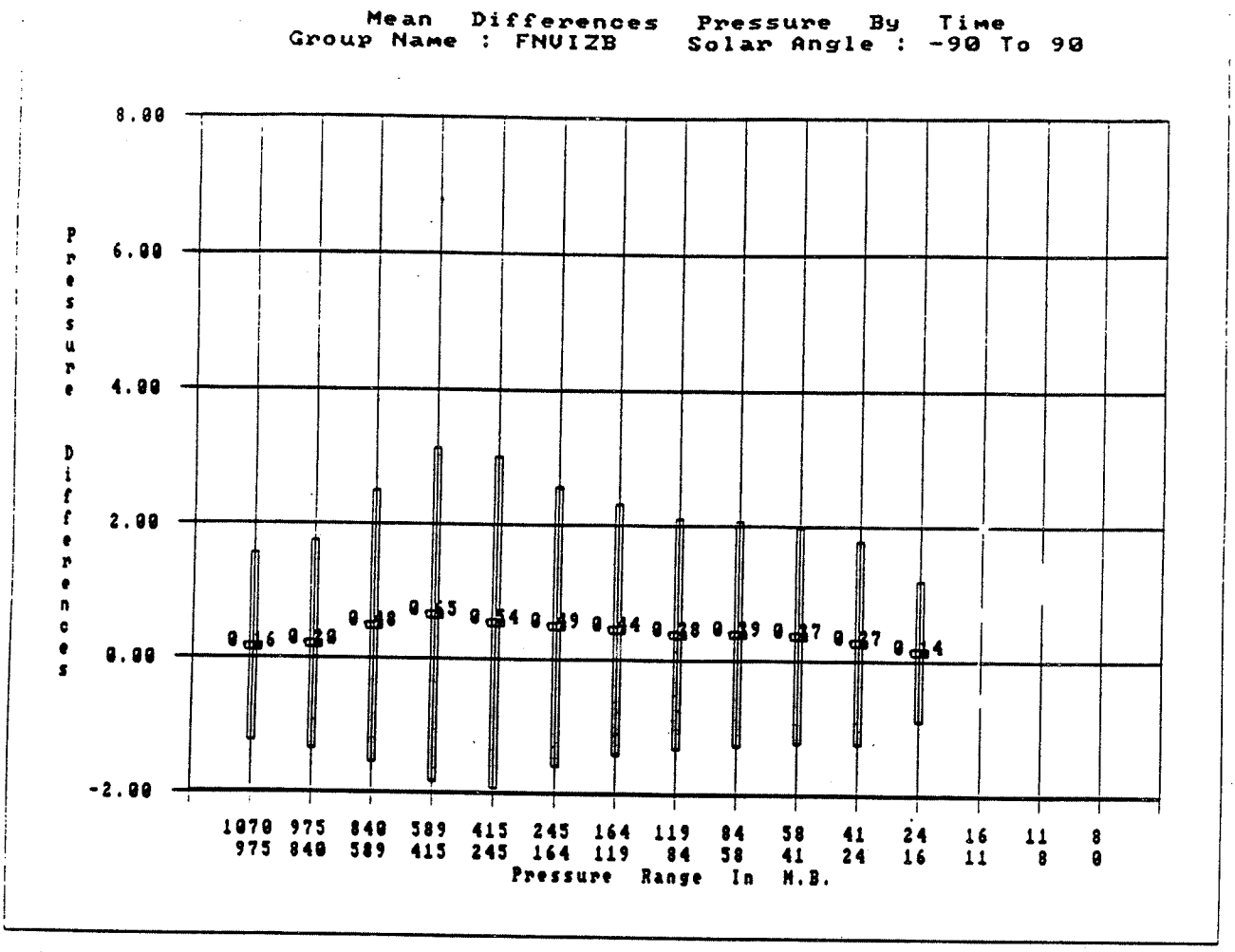

Figure 3. Mean/std. deviation of Pressure Difference within selected pressure layers. Plotted values are mean differences (mb). Bar gives +/- 1 std. deviation. Sampled at same time of flight.

FROM	MB.	TO	SAMPLE SIZE	# OF FLIGHTS	PRIMARY MEAN	SECONDARY MEAN	MEAN DIFF	RMS DIFF	STD DIFF
975.0	THRU	1069.9	17	13	988.56	988.39	.16	1.37	1.41
840.0	THRU	974.9	159	33	906.00	905.81	.20	1.57	1.56
589.0	THRU	839.9	341	33	707.88	707.40	.48	2.08	2.03
415.0	THRU	588.9	305	33	499.62	498.97	.65	2.57	2.49
245.0	THRU	414.9	410	32	325.70	325.15	.54	2.52	2.47
164.0	THRU	244.9	281	31	202.84	202.35	.49	2.14	2.08
119.0	THRU	163.9	202	29	140.29	139.85	.44	1.92	1.87
84.0	THRU	118.9	214	29	100.77	100.38	.38	1.76	1.73
58.9	THRU	83.9	196	28	71.03	70.64	.39	1.72	1.68
41.5	THRU	58.8	187	26	49.84	49.46	.37	1.65	1.62
24.5	THRU	41.4	210	24	32.69	32.42	.27	1.54	1.52
16.4	THRU	24.4	92	17	20.78	20.63	.14	1.06	1.05

Table 3. Mean, rms (functional precision), and std. dev. of Pressure Difference within selected pressure layers. Sampled at same time of flight.

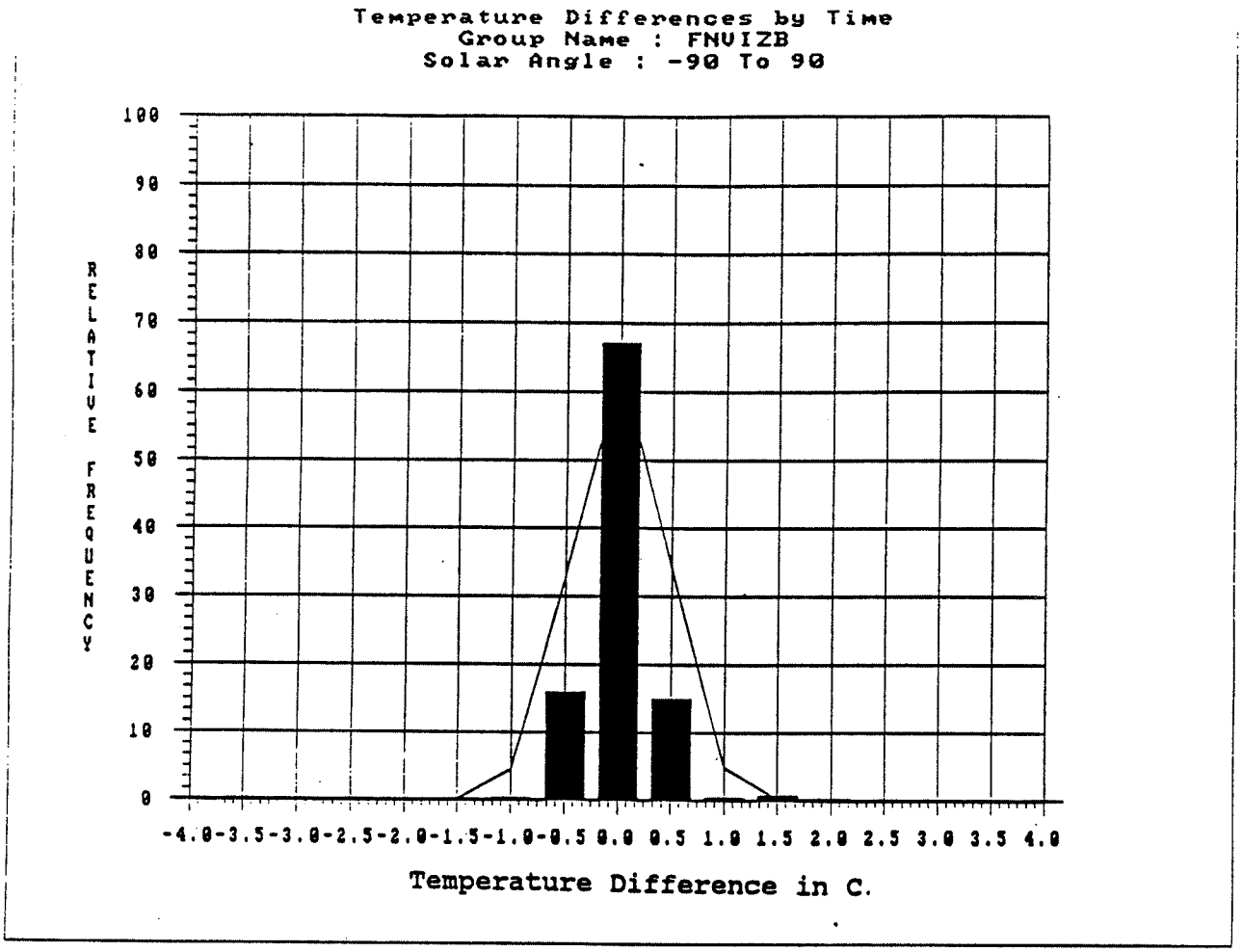

Figure 4. Histogram of Temperature Difference sampled at same time of flight. Normal curve computed from sample mean and std. dev.

DEG. FROM	TO	SAMPLE SIZE	# OF FLIGHTS	Absolute Temperature Difference Relative Frequency in % 0.0-0.5	0.6-1.0	1.1-1.5	1.6-2.0	2.1-2.5	2.6-3.0	> = 3.1	MEAN DIFF.	RMS DIFF.	STD.DEV. DIFF.
20.0	THRU 34.9	55	15	92.7	0.0	0.0	7.3	0.0	0.0	0.0	.14	.52	.51
5.0	THRU 19.9	206	28	94.7	1.0	1.0	3.4	0.0	0.0	0.0	.07	.39	.38
-5.0	THRU 4.9	249	33	96.8	.8	.8	1.6	0.0	0.0	0.0	.05	.32	.32
-20.0	THRU -5.1	272	33	96.7	1.1	1.8	.4	0.0	0.0	0.0	.04	.29	.29
-40.0	THRU -20.1	296	32	97.6	2.4	0.0	0.0	0.0	0.0	0.0	-.00	.25	.25
-60.0	THRU -40.1	1059	32	92.3	7.7	0.0	0.0	0.0	0.0	0.0	-.01	.31	.31
-90.0	THRU -60.1	480	26	94.4	5.6	0.0	0.0	0.0	0.0	0.0	-.04	.28	.28
	ALL	2617	33	94.3	4.7	.3	.6	0.0	0.0	0.0	.01	.31	.31

Table 4. Frequency of occurrence (%) of Absolute Temperature Difference within selected temperature intervals and for all data. Mean, rms (functional precision), and std. dev. of Temperature Difference for intervals and all data. Sampled at same time of flight.

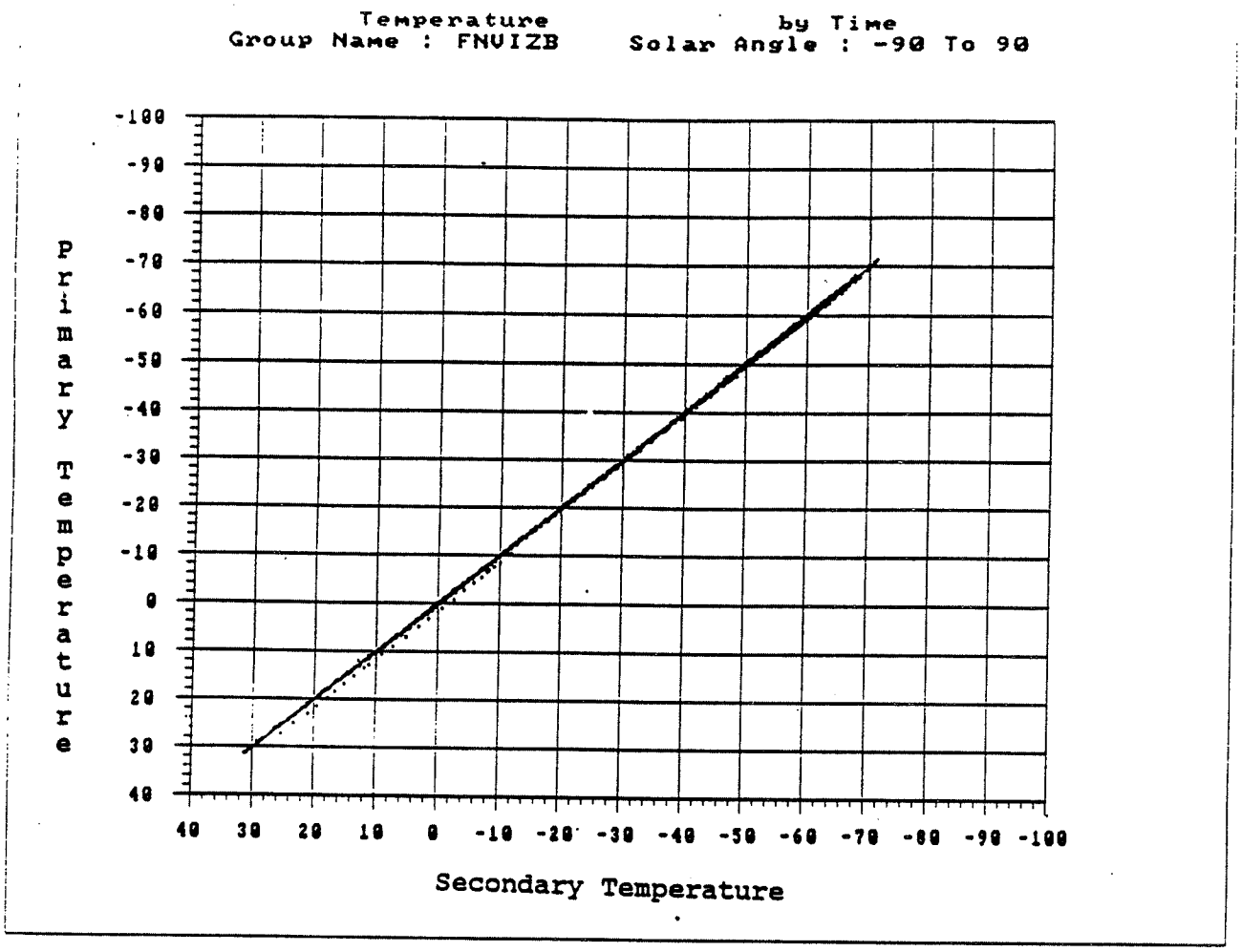

Figure 5. Scatter plot of 'primary sonde' Temperature versus 'secondary sonde' Temperature sampled at same time of flight. Regression line also plotted.

SAMPLE SIZE	# OF FLIGHTS	MEAN DIFF	STD DEV DIFF	RMS DIFF	SKEW. DIFF	KURT. DIFF	CORR. P & S	PRIM MIN	PRIM MAX	SECOND MIN	SECOND MAX	DIFFER MIN	DIFFER MAX
2617.0	33	.01	.31	.31	1.45	9.53	1.00	-71.50	31.20	-71.20	31.40	-1.00	2.00

Table 5. Temperature sampled at same time of flight. Mean, std. dev., rms, skewness, and kurtosis of differences. 'Primary sonde' and 'secondary sonde' correlation. Minimum and maximum Temperature and Temperature Difference in degrees C.

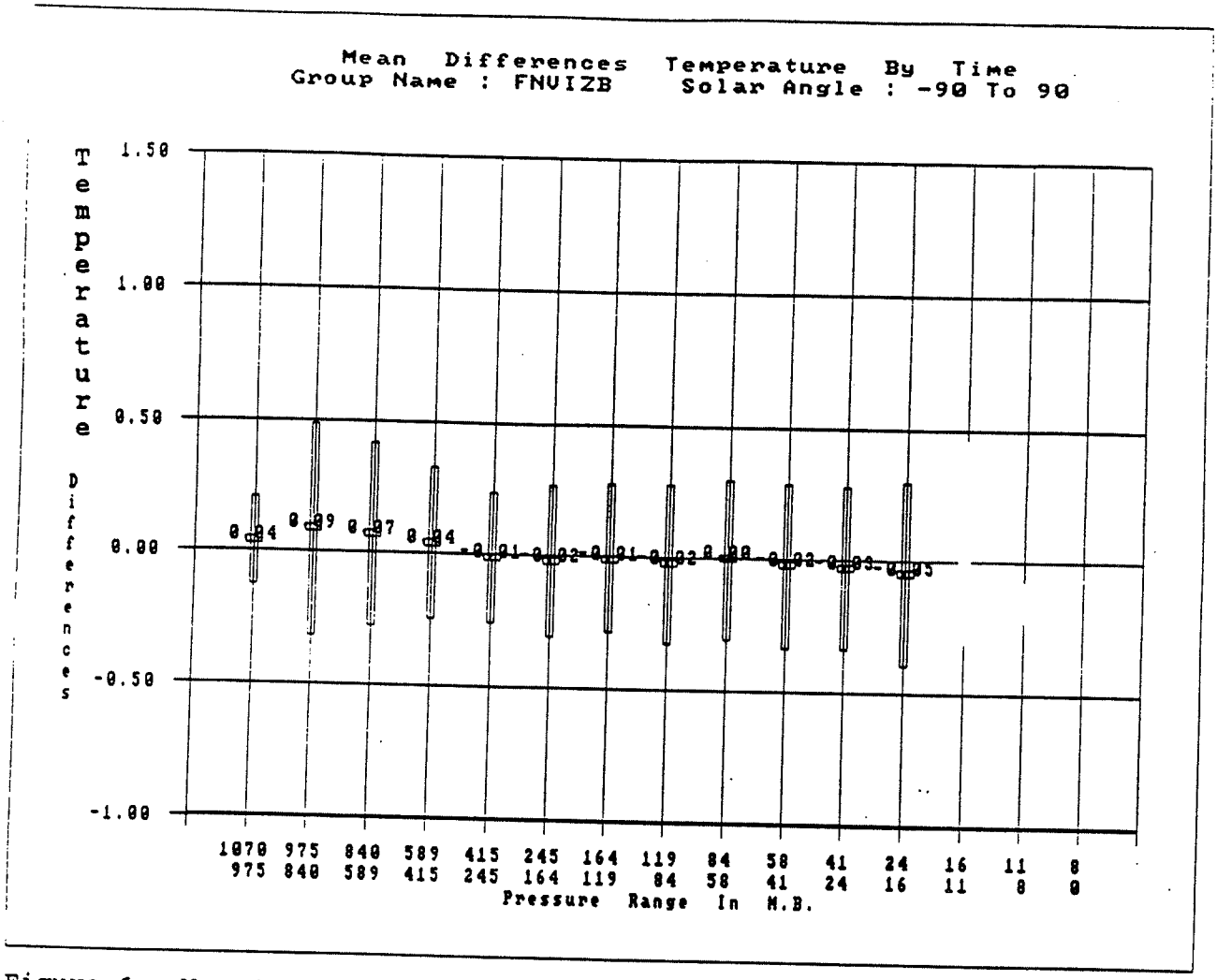

Figure 6. Mean/std. deviation of Temperature Difference within selected pressure layers. Plotted values are mean differences (deg. C). Bar gives +/- 1 std. deviation. Sampled at same time of flight.

FROM	MB.	TO	SAMPLE SIZE	# OF FLIGHTS	PRIMARY MEAN	SECONDARY MEAN	MEAN DIFF	RMS DIFF	STD DIFF
975.0	THRU	1069.9	17	13	12.18	12.14	.04	.17	.17
840.0	THRU	974.9	159	33	13.99	13.90	.09	.41	.40
589.0	THRU	839.9	341	33	2.49	2.42	.07	.35	.35
415.0	THRU	588.9	305	33	-13.50	-13.53	.04	.29	.29
245.0	THRU	414.9	410	32	-35.80	-35.79	-.01	.25	.25
164.0	THRU	244.9	281	31	-55.58	-55.56	-.02	.29	.29
119.0	THRU	163.9	202	29	-60.62	-60.62	-.01	.28	.28
84.0	THRU	118.9	214	29	-61.98	-61.96	-.02	.30	.30
58.9	THRU	83.9	196	28	-60.68	-60.67	-.00	.31	.31
41.5	THRU	58.8	167	26	-57.98	-57.96	-.02	.31	.31
24.5	THRU	41.4	210	24	-54.22	-54.19	-.03	.31	.31
16.4	THRU	24.4	92	17	-50.15	-50.10	-.05	.35	.35

Table 6. Mean, rms (functional precision), and std. dev. of Temperature Difference within selected pressure layers. Sampled at same time of flight.

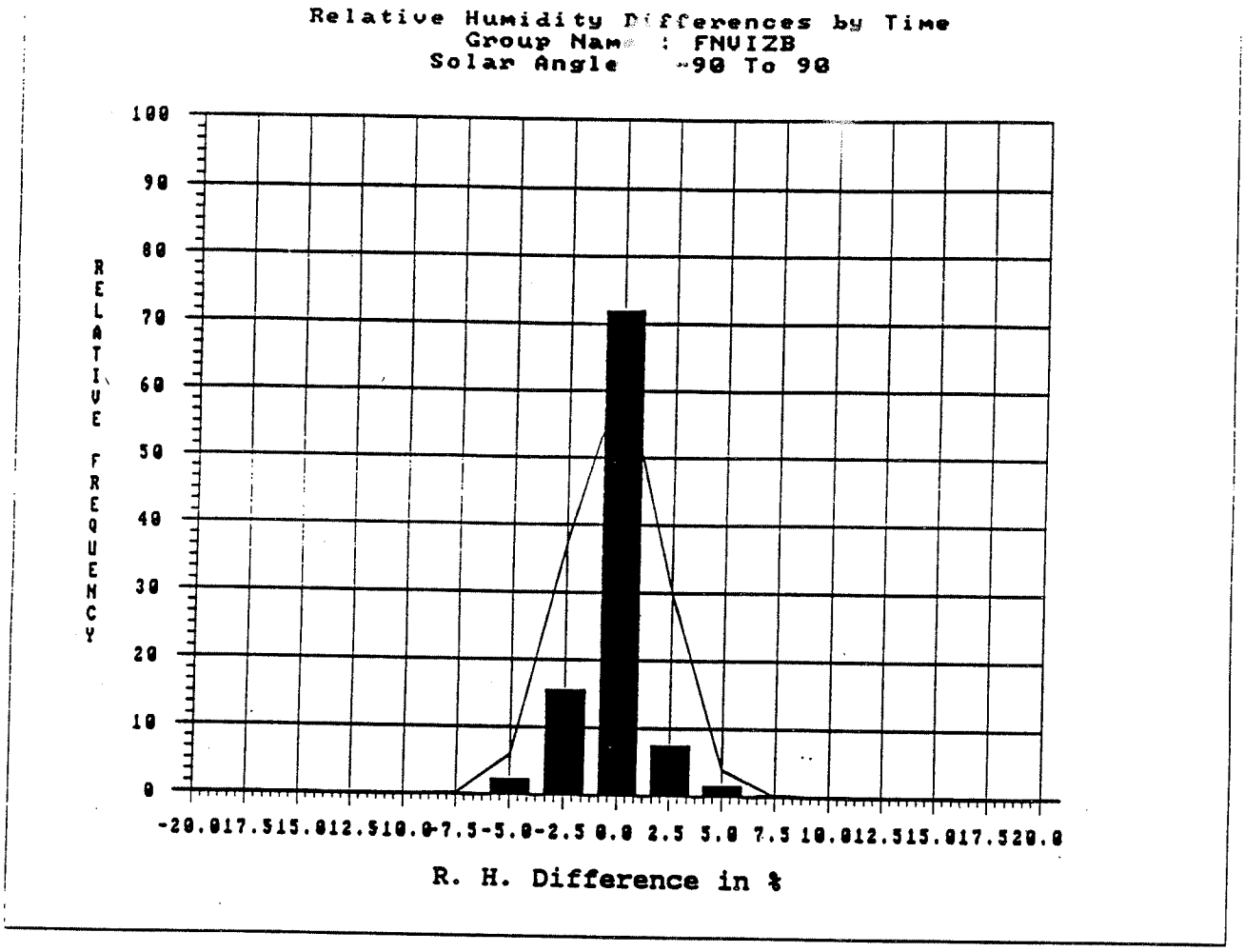

Figure 7. Histogram of Relative Humidity Difference sampled at same time of flight. Normal curve computed from sample mean and std. dev.

FROM	PERC	TO	SAMPLE SIZE	# OF FLIGHTS	Absolute R. H. Difference Interval 0.0-2.5	2.6-5.0	5.1-7.5	7.6-10.0	10.1-12.5	12.6-15.0	> = 15.1	MEAN DIFF.	RMS DIFF.	STD.DEV. DIFF.
					Relative Frequency in %									
90.0	THRU	100.0	127	16	100.0	0.0	0.0	0.0	0.0	0.0	0.0	-.05	.50	.50
80.0	THRU	89.9	97	21	97.9	2.1	0.0	0.0	0.0	0.0	0.0	-.19	.99	.98
70.0	THRU	79.9	80	21	95.0	5.0	0.0	0.0	0.0	0.0	0.0	-.12	1.11	1.11
60.0	THRU	69.9	127	29	99.2	.8	0.0	0.0	0.0	0.0	0.0	-.23	1.12	1.10
50.0	THRU	59.9	108	29	98.1	1.9	0.0	0.0	0.0	0.0	0.0	-.27	.95	.92
40.0	THRU	49.9	74	26	93.2	6.8	0.0	0.0	0.0	0.0	0.0	-.27	1.30	1.28
30.0	THRU	39.9	87	24	86.2	10.3	2.3	1.1	0.0	0.0	0.0	-.06	2.01	2.02
20.0	THRU	29.9	97	24	56.7	28.9	12.4	2.1	0.0	0.0	0.0	-.21	3.36	3.37
10.0	THRU	19.9	277	23	90.6	8.3	1.1	0.0	0.0	0.0	0.0	-.32	1.49	1.46
	ALL		1078	33	91.3	6.9	1.6	.3	0.0	0.0	0.0	-.20	1.58	1.56

Table 7. Frequency of occurrence (%) of Absolute Relative Humidity Difference within selected relative humidity intervals and for all data. Mean, rms (functional precision), and std. dev. of Relative Humidity Difference for layers and all data. Sampled at same time of flight.

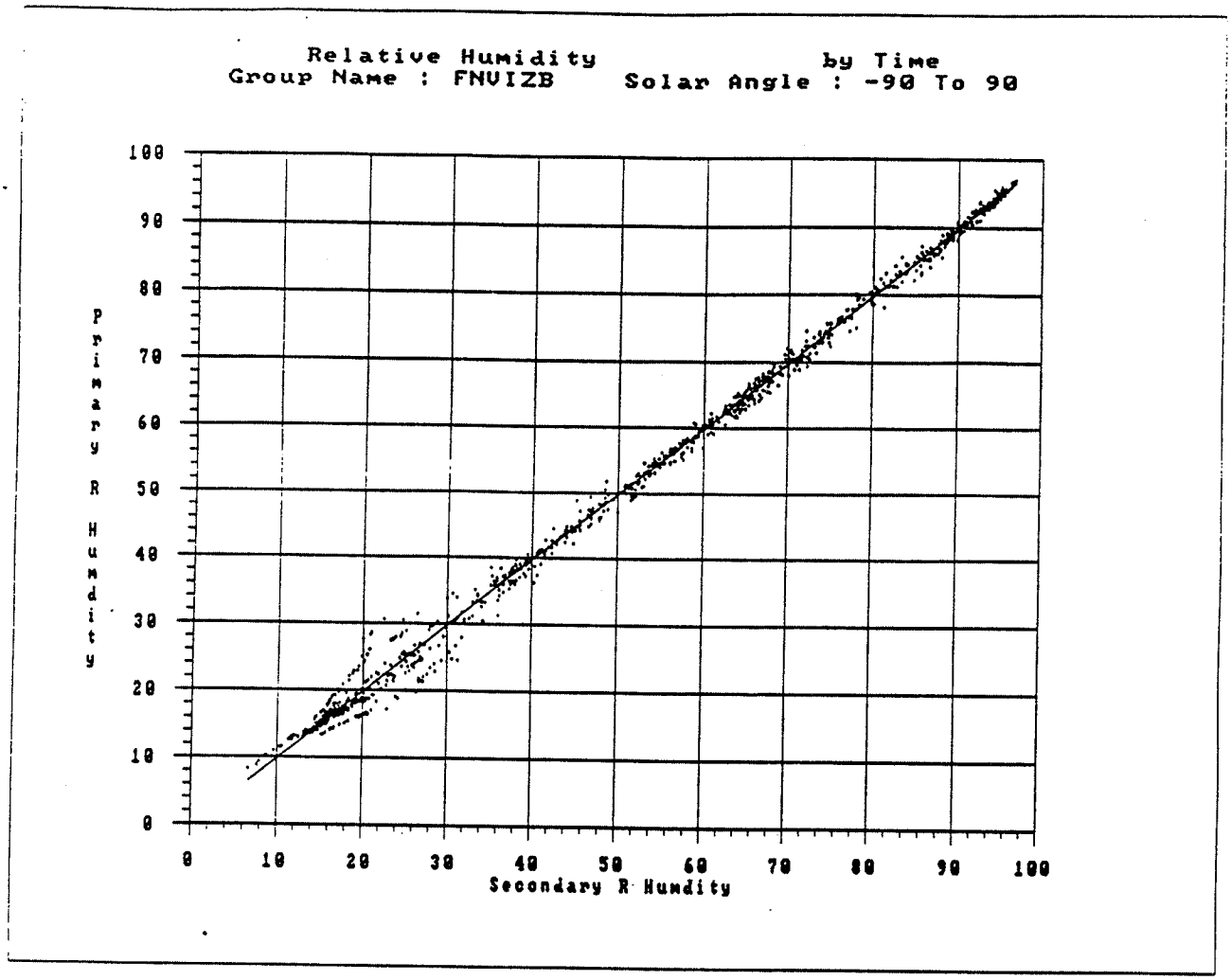

Figure 8. Scatter plot of 'primary sonde' Relative Humidity versus 'secondary sonde' Relative Humidity sampled at same time of flight. Regression line also plotted.

SAMPLE SIZE	# OF FLIGHTS	MEAN DIFF	STD DEV DIFF	RMS DIFF	SKEW. DIFF	KURT. DIFF	CORR. P & S	PRIM MIN	PRIM MAX	SECOND MIN	SECOND MAX	DIFFER MIN	DIFFER MAX
1078.0	33	-.20	1.56	1.58	.17	7.58	1.00	8.30	97.10	6.70	96.90	-6.70	8.20

Table 8. Relative Humidity sampled at same time of flight. Mean, std. dev., rms, skewness, and kurtosis of differences. 'Primary sonde' and 'secondary sonde' correlation. Minimum and maximum Relative Humidity Difference in percent.

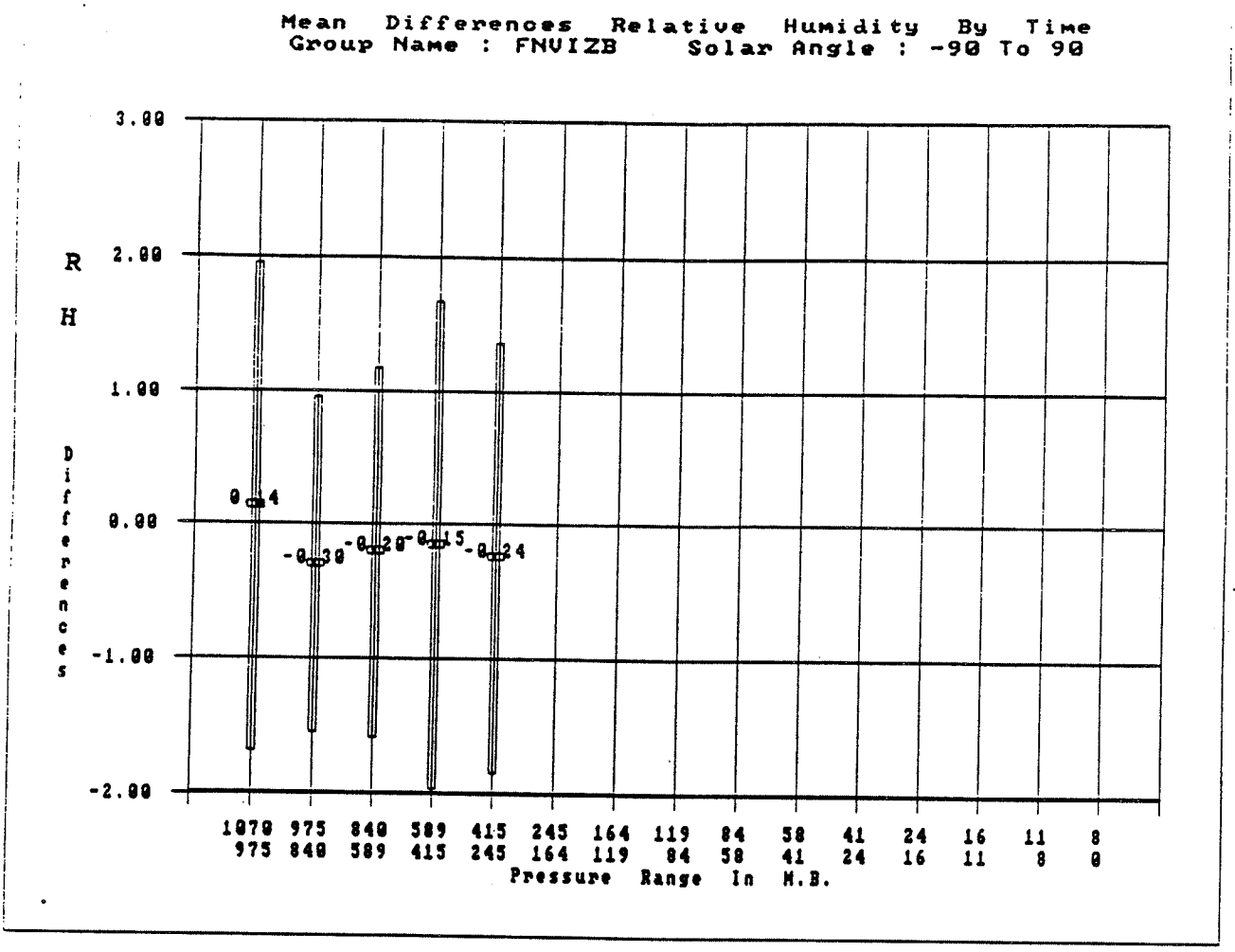

Figure 9. Mean/std. deviation of Relative Humidity Difference within selected pressure layers. Plotted values are mean differences (%R.H.). Bar gives +/- 1 std. deviation. Sampled at same time of flight.

FROM	MB.	TO	SAMPLE SIZE	# OF FLIGHTS	PRIMARY MEAN	SECONDARY MEAN	MEAN DIFF	RMS DIFF	STD DIFF
975.0	THRU	1069.9	17	13	60.06	59.93	.14	1.78	1.83
840.0	THRU	974.9	159	33	61.56	61.86	-.30	1.29	1.25
589.0	THRU	839.9	341	33	57.56	57.76	-.20	1.40	1.38
415.0	THRU	588.9	304	33	44.57	44.72	-.15	1.83	1.83
245.0	THRU	414.9	257	31	37.20	37.44	-.24	1.63	1.61

Table 9. Mean, rms (functional precision), and std. dev. of Relative Humidity Difference within selected pressure layers. Sampled at same time of flight.

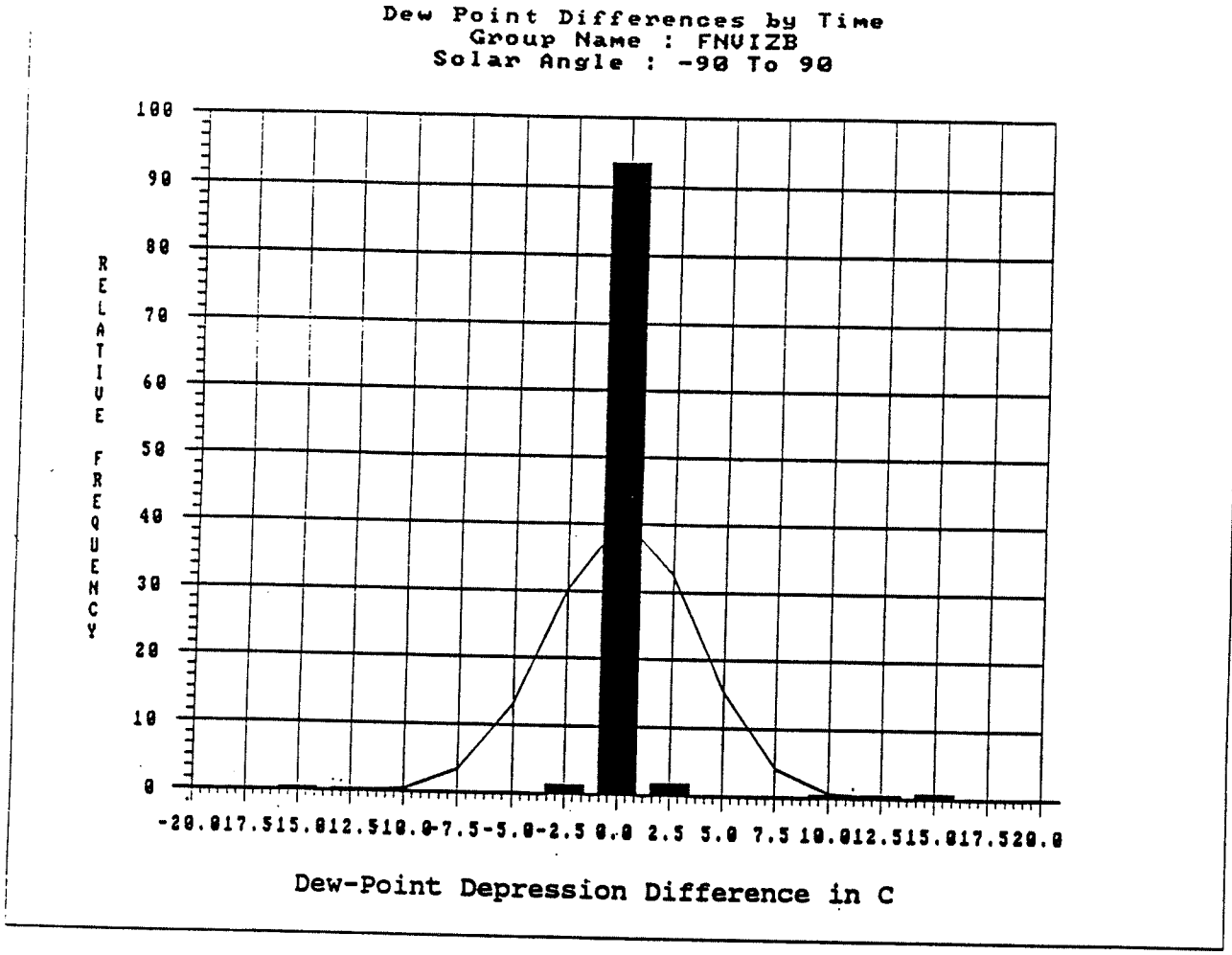

Figure 10. Histogram of Dew-Point Depression Difference sampled at same time of flight. Noraml curve computed from sample mean and std. dev.

SAMPLE SIZE	# OF FLIGHTS	MEAN DIFF	STD DEV DIFF	RMS DIFF	SKEW. DIFF	KURT. DIFF	CORR. P & S	PRIM MIN	PRIM MAX	SECOND MIN	SECOND MAX	DIFFER MIN	DIFFER MAX
1078.0	33	.17	2.44	2.44	1.04	33.72	.98	.50	30.00	.50	30.00	-17.80	16.50

Table 10. Dew-Point Depression sampled at same time of flight. Mean, std. dev., rms (functional precision), skewness, and kurtosis of differences. 'Primary sonde' and 'secondary sonde' correlation. Minimum and maximum Dew-Point Depression and Dew-Point Depression Difference in degrees C.

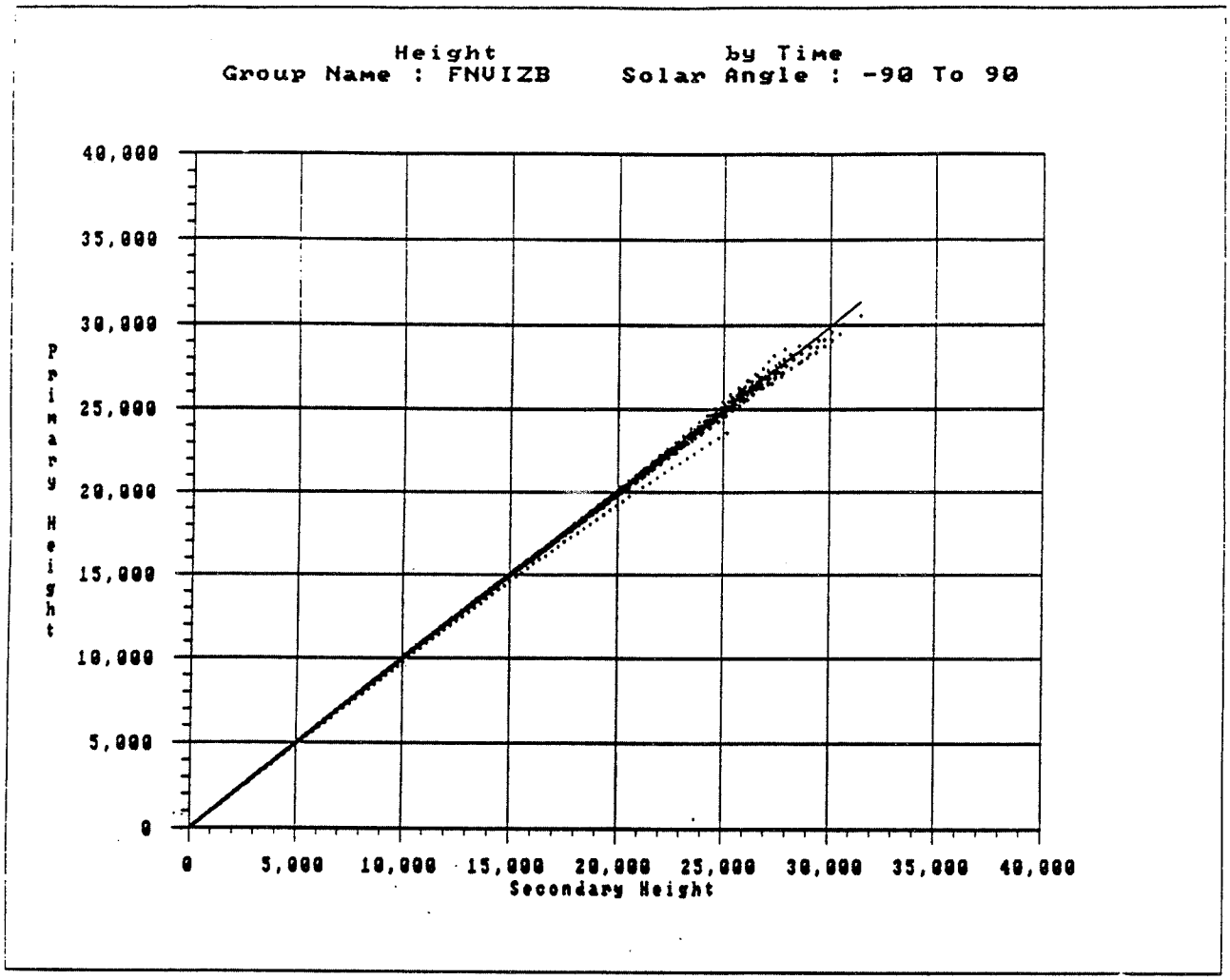

Figure 11. Scatter plot of 'primary sonde' Height versus 'secondary sonde' Height sampled at same time of flight. Regression line also plotted.

SAMPLE SIZE	# OF FLIGHTS	MEAN DIFF	STD DEV DIFF	RMS DIFF	SKEW. DIFF	KURT. DIFF	CORR. P & S	PRIM MIN	PRIM MAX	SECOND MIN	SECOND MAX	DIFFER MIN	DIFFER MAX
2617.0	33	-27.14	158.55	160.86	-3.03	24.47	1.00	91.20	30544.1	91.50	31447.1	-1580.3	828.90

Table 11. Height sampled at same time of flight. Mean, std. dev., rms, skewness, and kurtosis of differences. 'Primary sonde' and 'secondary sonde' correlation. Minimum and maximum Height Difference in meters.

5. COMPARISON BY PRESSURE

Comparisons by pressure are more useful to the operational meteorologist since they represent the functional precision of radiosonde data at a specific pressure levels. The derived statistics can be directly applied to constant-pressure analysis and forecast model initialization. For dual flights, two radiosondes can report different pressures at the same time if their baroswitches have different response characteristics. By comparing the temperature, relative humidity, or dew point depression at the same pressure, values at slightly different times will be used and different statistics will be produced. For example, a 1 mb pressure difference near the surface will result in an approximate 2 second time difference, but at 10 mb an approximate 1 minute time difference results. This time difference contributes to the overall measurement differences and, consequently, tend toward worse precisions (larger RMSD) for temperature and relative humidity.

However, height precisions by pressure are significantly better than precisions by time. This is because height is not directly measured by the radiosonde but is derived using the hypsometric equation and, therefore, is a function of its measured pressure and mean virtual temperature. Comparing height calculations from measurements made by two sondes at the same time, the height discrepancies are caused by the differences in measured pressures and mean virtual temperatures. However, if height calculations using measurements made at the same pressure are compared, no difference in measured pressures occur and only the difference in mean virtual temperatures remains. Since the mean virtual temperature calculation is insensitive to small time differences when the sondes measure a common pressure, the discrepancies in heights compared by pressure are significantly less than those compared by time and, consequently, the functional precision is better (smaller RMSD).

5.1 TEMPERATURE

For the total population, 94.6% of the temperature differences by pressure were within ±1.0°C, 99.6% were within ±2.5°C, and only 0.2% exceeded ±3.0°C (Figure 12, Table 12). As was done for temperatures compared by time, relative frequencies for the magnitude of temperature difference occurring within a difference interval are given for 7 temperature intervals (Table 12)

The scatter plot (Figure 13) shows a small increase in scatter at colder temperatures. This would be expected since the time differences between points compared by pressure tend to be larger at higher altitudes.

The overall functional precision (RMSD) of temperature by pressure is 0.54°C (Table 12). For the 7 temperature intervals, precisions (RMSD) ranged from 0.33°C between 5 and 20°C to 0.77°C between -90 and -60°C. For all temperature intervals, sample sizes are small (15 to 33) and the statistics should be used with caution.

Precisions and other statistics for various pressure levels were computed (Table 18a).

5.2 HUMIDITY

Relative humidity is measured by the radiosonde hygristor in terms of electrical resistance. It is converted to dew-point depressions for message coding and transmission to other users. To determine a measure of humidity from the dew-point depression, the temperature must be known, so, if the temperatures reported by both sondes used in the comparisons are not the same, the dew-point depression differences do not give a pure measure of the humidity statistics but rather a combined measure of temperature and humidity statistics which are difficult to objectively analyze.

5.2.1 RELATIVE HUMIDITY

For the total population, 93.6% of the relative humidity differences by pressure were within ±5% RH (Figure 14, Table 14).

The scatter plot (Figure 15) is similar to that for data compared at the same time (Figure 8). As stated earlier, accuracies of relative humidities below 20% RH calculated using current NWS equations is questionable so the precision at these values may not reflect optimal performance.

Overall functional precision (RMSD) for relative humidity by pressure is 2.3% RH (Table 14). Precision and other statistics for various pressure levels were computed (Table 18b).

5.2.2 DEW-POINT DEPRESSION

Overall functional precision (RMSD) for dew-point depression by pressure is 2.66°C (Table 16). Refer to section 4.3.2 for comments on the validity of these precision numbers.

5.3 HEIGHT

The scatter plot contains no outlier points indicating a high degree of precision throughout the range of heights (Figure 17). The scatter plot of heights by time (Figure 11) shows significantly more scatter. Good height precision is important to meteorological operations since numerical models are highly sensitive to inconsistencies in radiosonde calculations of pressure-level heights that are used to initialize them.

The overall functional precision (RMSD) for the height by pressure is 15.3 meters (Table 17). Precision and other statistics for various pressure levels were computed (Table 18c). These statistics are based on small sample sizes and should be used with caution. However, each sample is totally independent since each comes from a different flight. Below 900 mb, the precision of the pressure heights is better than 1 meter. Above the 900 mb level, the height precisions of pressure levels reach 10 meters near 300 mb, 20 meters near 100 mb, 25 meters near 40 mb, and 30 meters near 20 mb.

Comparing the magnitude of height difference with height produced a strong correlation of 0.58 (i.e., more height scatter at greater heights).

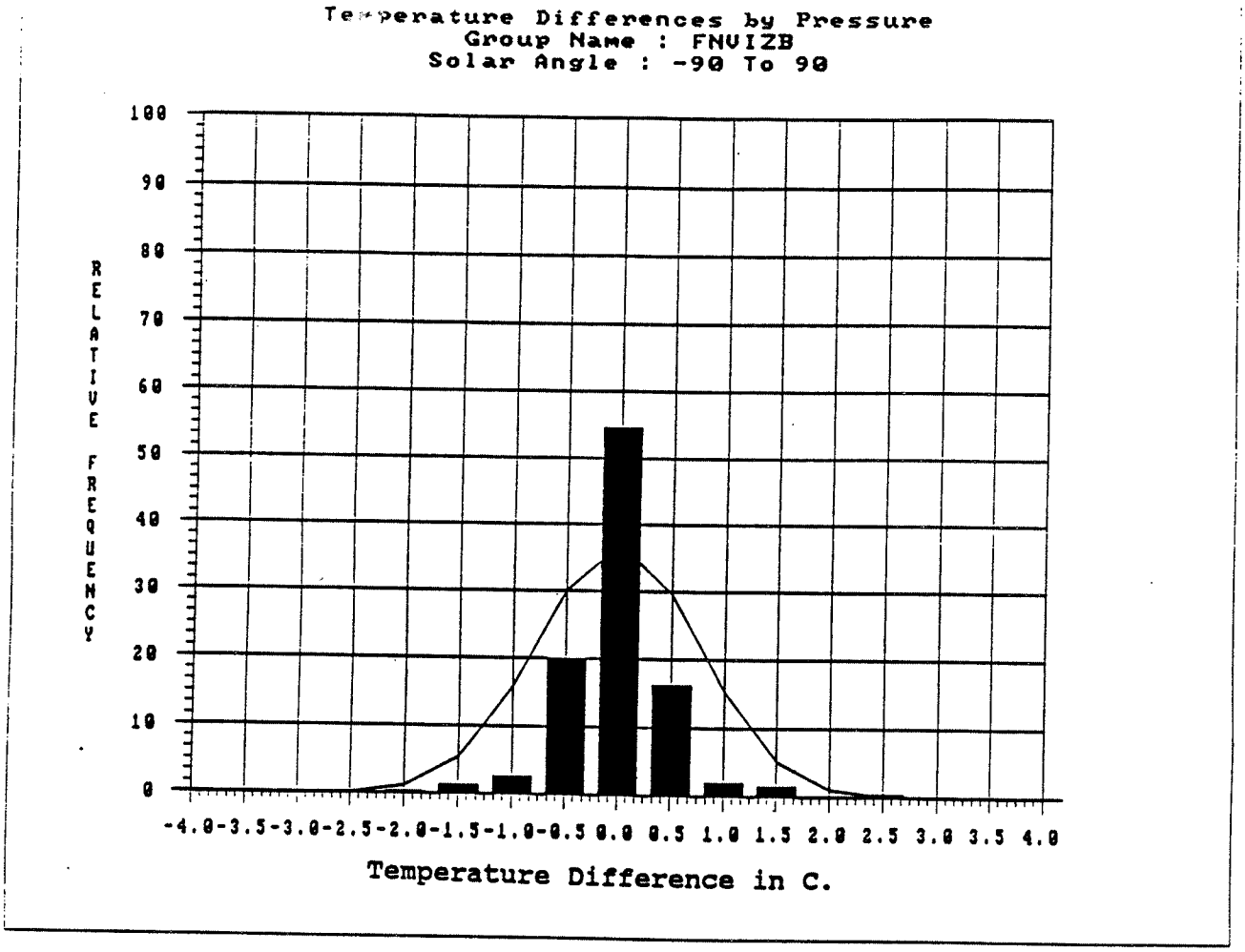

Figure 12. Histogram of Teperature Difference sampled at same pressure. Noral curve computed from sample mean and standard deviation.

DEG. FROM	TO	SAMPLE SIZE	# OF FLIGHTS	Absolute Temperature Difference 0.0-0.5	0.6-1.0	1.1-1.5	1.6-2.0	2.1-2.5	2.6-3.0	> = 3.1	MEAN DIFF.	RMS DIFF.	STD.DEV. DIFF.
				Relative Frequency in %									
20.0	THRU 34.9	27	15	92.6	0.0	3.7	3.7	0.0	0.0	0.0	-.03	.47	.47
5.0	THRU 19.9	58	27	91.4	6.9	0.0	1.7	0.0	0.0	0.0	-.01	.33	.33
-5.0	THRU 4.9	58	33	93.1	3.4	1.7	1.7	0.0	0.0	0.0	.03	.38	.38
-20.0	THRU -5.1	65	33	92.3	4.6	3.1	0.0	0.0	0.0	0.0	-.00	.34	.35
-40.0	THRU -20.1	44	32	86.4	9.1	4.5	0.0	0.0	0.0	0.0	-.09	.45	.44
-60.0	THRU -40.1	227	32	75.8	18.9	3.1	1.3	.4	.4	0.0	-.04	.56	.56
-90.0	THRU -60.1	101	25	71.3	18.8	5.9	1.0	2.0	0.0	1.0	.06	.77	.77
	ALL	580	33	81.7	12.9	3.3	1.2	.5	.2	.2	-.01	.54	.54

Table 12. Frequency of occurrence (%) of Absolute Temperature Difference within selected temperature intervals and for all data. Mean, rms (functional precision), and std. dev. of Temperature Difference for layers and all data. Sampled at same pressure.

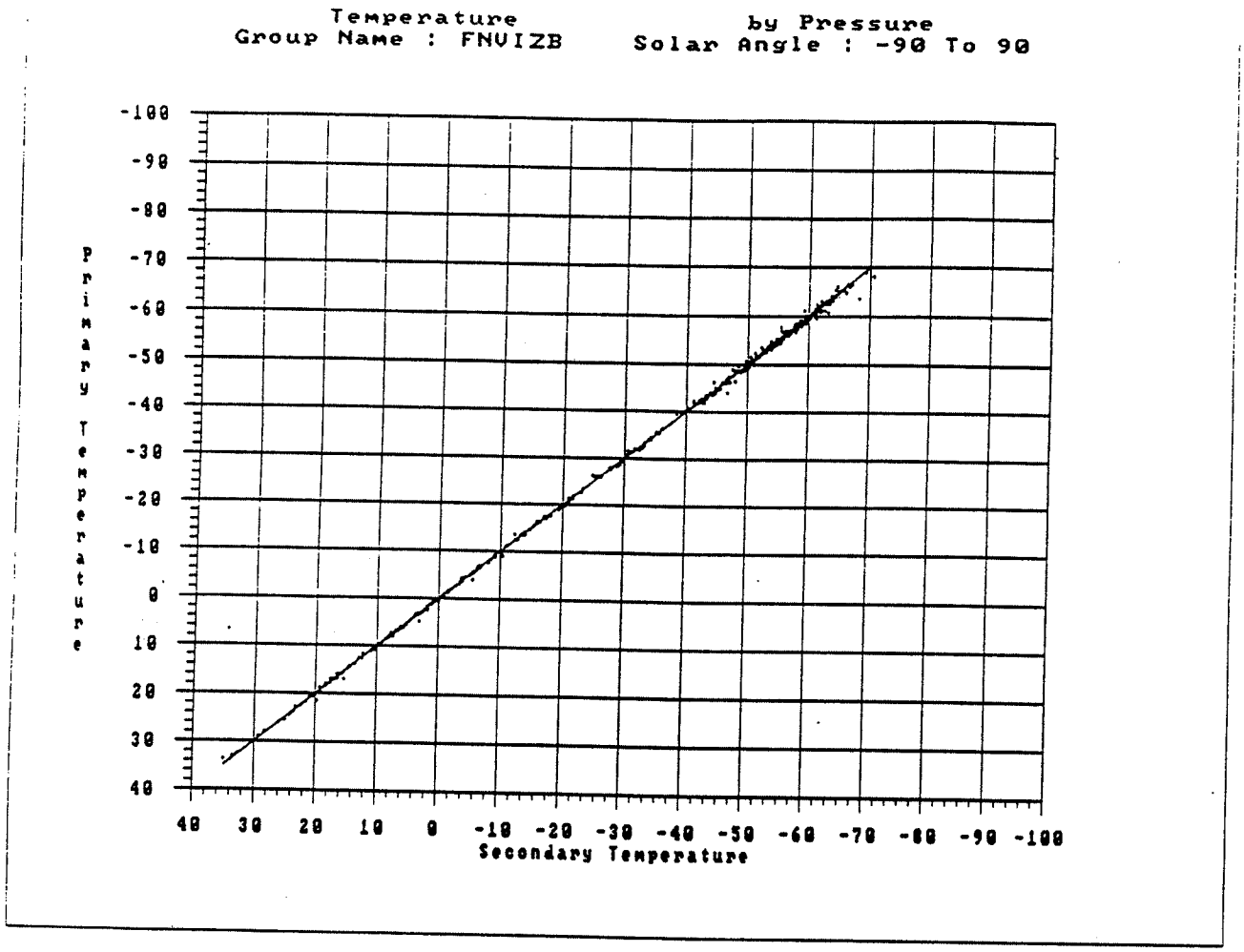

Figure 13. Scatter plot of 'primary sonde' Temperature versus 'secondary sonde' Temperature sampled at same pressure. Regression line also plotted.

SAMPLE SIZE	# OF FLIGHTS	MEAN DIFF	STD DEV DIFF	RMS DIFF	SKEW. DIFF	KURT. DIFF	CORR. P & S	PRIM MIN	PRIM MAX	SECOND MIN	SECOND MAX	DIFFER MIN	DIFFER MAX
580.00	33	-.01	.54	.54	1.30	15.74	1.00	-70.20	33.60	-70.60	34.90	-2.50	4.60

Table 13. Temperature sampled at same pressure. Mean, std. dev., rms, skewness, and kurtosis of differences. 'Primary sonde' and 'secondary sonde' correlation. Minimum and maximum Temperature and Temperature Difference in degrees C.

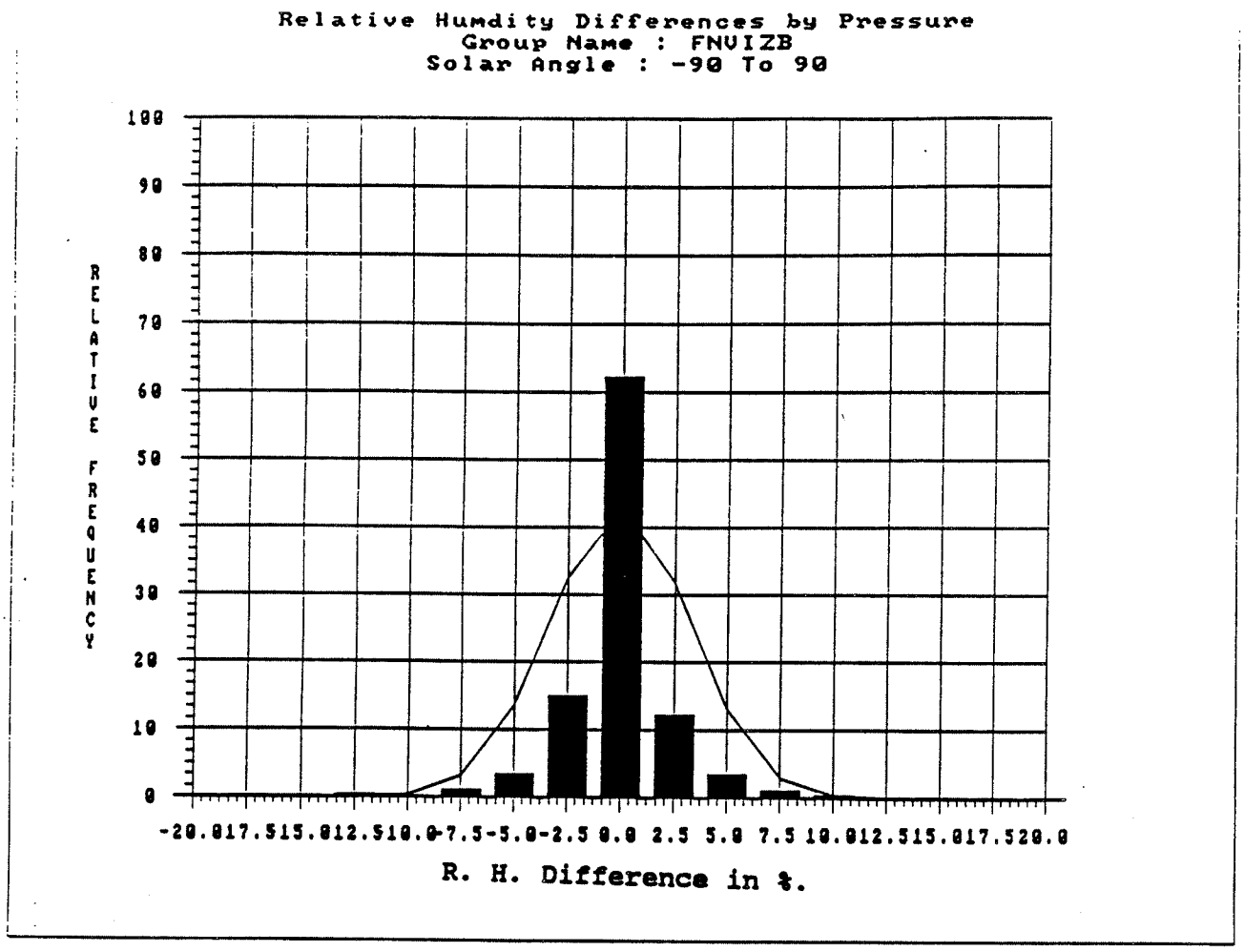

Figure 14. Histogram of Relative Humidity Difference sampled at same pressure. Normal curve computed from sample mean and std. dev.

FROM	PERC	TO	SAMPLE SIZE	# OF FLIGHTS	Absolute R. H. Difference Interval 0.0-2.5	2.6-5.0	5.1-7.5	7.6-10.0	10.1-12.5	12.6-15.0	> = 15.0	MEAN DIFF.	RMS DIFF.	STD.DEV. DIFF.
					Relative Frequency in %									
90.0	THRU	100.0	40	15	100.0	0.0	0.0	0.0	0.0	0.0	0.0	-.04	.61	.61
80.0	THRU	89.9	20	12	95.0	0.0	0.0	5.0	0.0	0.0	0.0	.52	2.18	2.17
70.0	THRU	79.9	21	14	90.5	0.0	9.5	0.0	0.0	0.0	0.0	.07	2.28	2.34
60.0	THRU	69.9	23.	13	100.0	0.0	0.0	0.0	0.0	0.0	0.0	-.01	.93	.95
50.0	THRU	59.9	29	17	89.7	6.9	0.0	0.0	3.4	0.0	0.0	.12	2.59	2.63
40.0	THRU	49.9	22	15	77.3	9.1	13.6	0.0	0.0	0.0	0.0	.14	2.63	2.69
30.0	THRU	39.9	22	16	77.3	13.6	9.1	0.0	0.0	0.0	0.0	.18	2.65	2.70
20.0	THRU	29.9	18	9	44.4	38.9	11.1	0.0	5.6	0.0	0.0	-.22	4.43	4.56
10.0	THRU	19.9	55	18	87.3	5.5	7.3	0.0	0.0	0.0	0.0	-.62	2.15	2.08
	ALL		252	33	86.9	6.7	5.2	.4	.8	0.0	0.0	-.06	2.32	2.32

Table 14. Frequency of occurrence (%) of Absolute Relative Humidity Difference within selected relative humidity intervals and for all data. Mean, rms (functional precision), and std. dev. of Relative Humidity Difference for layers and all data. Sampled at same pressure.

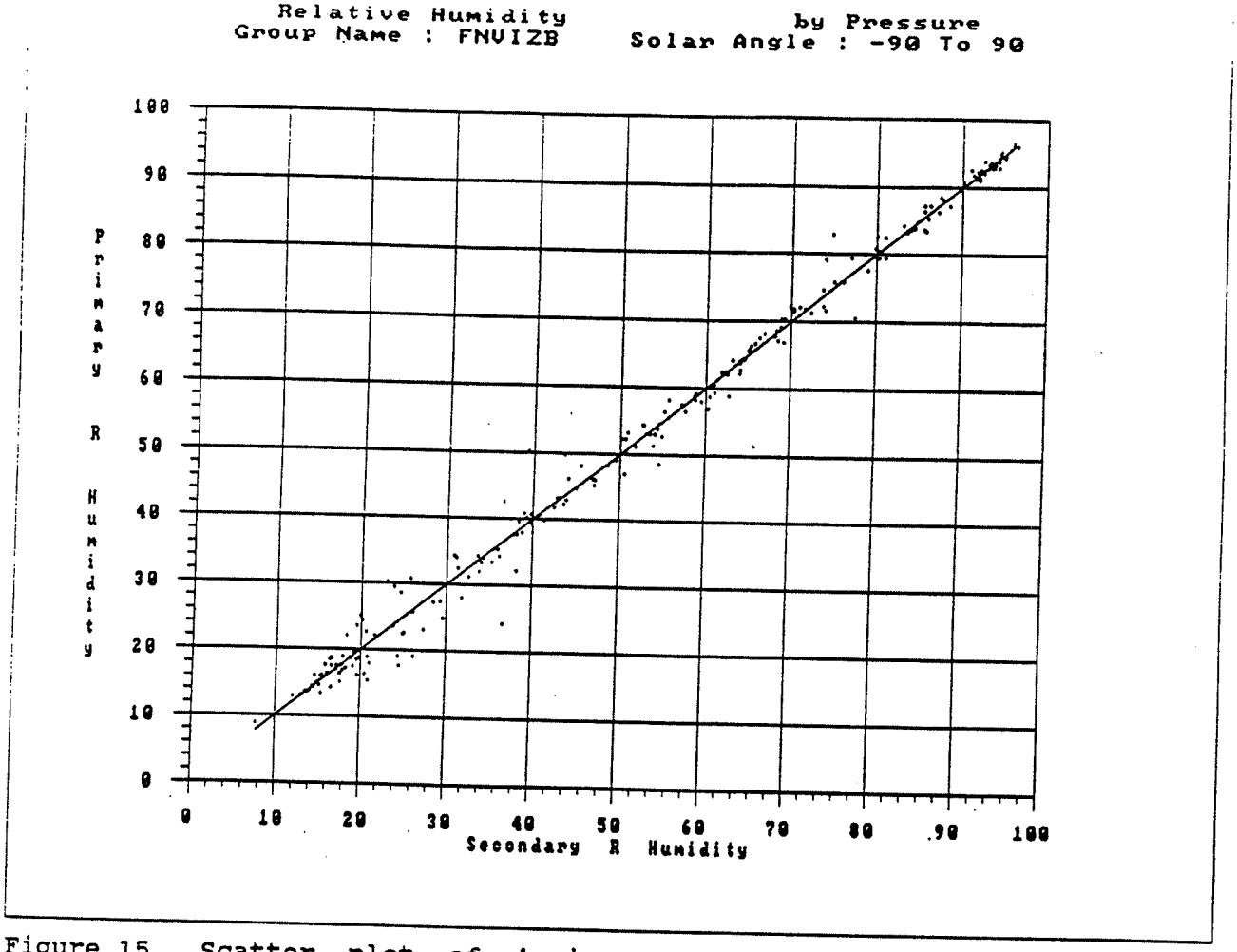

Figure 15. Scatter plot of 'primary sonde' Relative Humidity versus 'secondary sonde' Relative Humidity sampled at same pressure. Regression line also plotted.

SAMPLE SIZE	# OF FLIGHTS	MEAN DIFF	STD DEV DIFF	RMS DIFF	SKEW. DIFF	KURT. DIFF	CORR. P & S	PRIM MIN	PRIM MAX	SECOND MIN	SECOND MAX	DIFFER MIN	DIFFER MAX
252.00	33	-.06	2.31	2.32	-.12	9.22	1.00	8.90	96.50	7.70	96.50	-12.50	10.90

Table 15. Relative Humidity sampled at same pressure. Mean, std. dev., rms, skewness, and kurtosis of differences. 'Primary sonde' and 'secondary sonde' correlation. Minimum and maximum Relative Humidity and Relative Humidity Difference in percent.

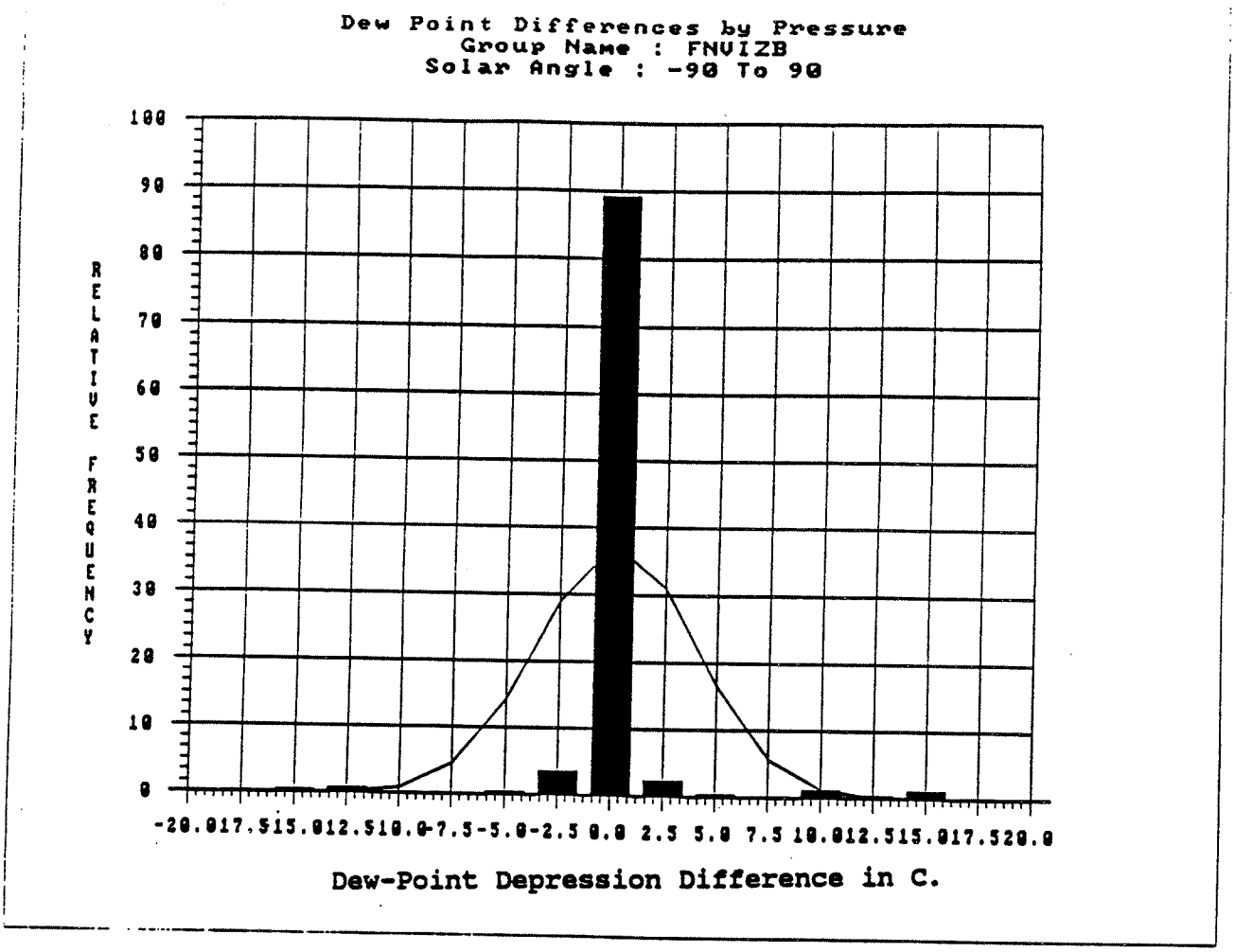

Figure 16. Histogram of Dew-Point Depression Difference sampled at same pressure. Normal curve computed from sample mean and std. dev.

SAMPLE SIZE	# OF FLIGHTS	MEAN DIFF	STD DEV DIFF	RMS DIFF	SKEW. DIFF	KURT. DIFF	CORR. P & S	PRIM MIN	PRIM MAX	SECOND MIN	SECOND MAX	DIFFER MIN	DIFFER MAX
252.00	33	.20	2.65	2.66	1.62	23.72	.97	.60	30.00	.60	30.00	-14.10	15.50

Table 16. Dew-Point Depression sampled at same pressure. Mean, std. dev., rms, skewness, and kurtosis of differences. 'Primary sonde' and 'secondary sonde' correlation. Minimum and maximum Dew-Point Depression and Dew-Point Depression Difference in degrees C.

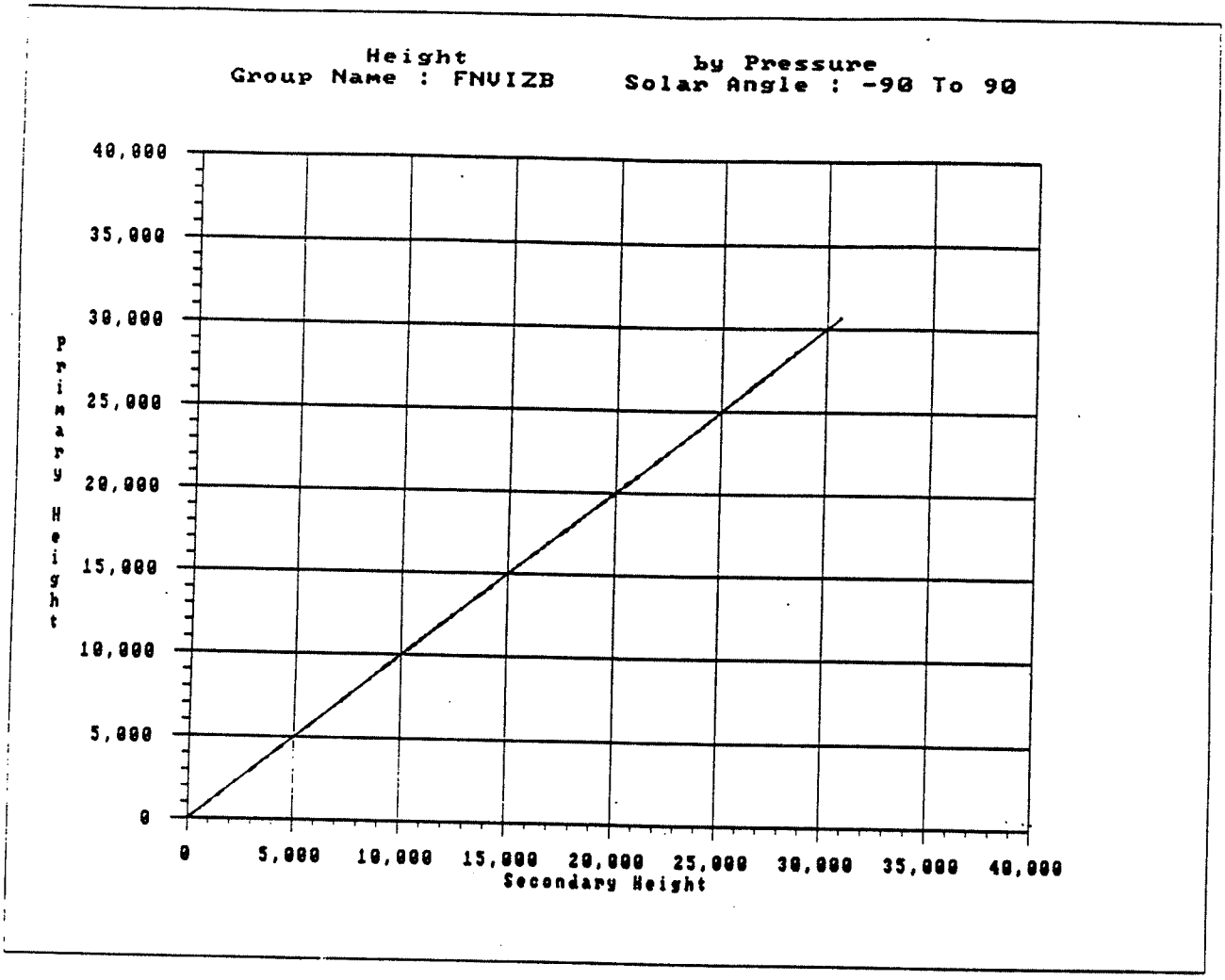

Figure 17. Scatter plot of 'primary sonde' Height versus 'secondary sonde' Height sampled at same pressure. Regression line also plotted.

SAMPLE SIZE	# OF FLIGHTS	MEAN DIFF	STD DEV DIFF	RMS DIFF	SKEW. DIFF	KURT. DIFF	CORR. P & S	PRIM MIN	PRIM MAX	SECOND MIN	SECOND MAX	DIFFER MIN	DIFFER MAX
580.00	33	-2.19	15.09	15.25	-.23	6.31	1.00	91.20	30679.8	91.50	30648.5	-63.90	58.60

Table 17. Height sampled at same pressure. Mean, std. dev., rms, skewness, and kurtosis of differences. 'Primary sonde' and 'secondary sonde' correlation. Minimum and maximum Height and Height Difference in meters.

Table 18 a.

VIZB Temperature Sensor Functional Precision Statistics at Various Pressure Levels

Pressure (mb)	Sample Size	Temperature Difference: [RMS	Kurt	Absolute Max]	Temperature Range:
1000	23	.40	4.81	1.3	34.9 to 0.7
900	28	.40	11.41	1.7	25.2 to -3.4
850	32	.35	12.71	1.6	20.5 to -1.6
700	33	.36	13.92	1.7	11.0 to -14.0
600	33	.38	7.91	1.5	2.9 to -21.6
500	33	.41	6.39	1.3	-5.1 to -32.7
400	32	.42	5.57	1.5	-15.3 to -43.6
300	32	.44	2.89	1.1	-30.3 to -48.7
250	31	.50	3.57	1.5	-40.1 to -56.1
200	30	.63	3.88	2.0	-48.6 to -66.4
150	29	.52	4.11	1.1	-49.2 to -69.3
100	29	.55	3.28	1.3	-51.7 to -70.2
80	28	.59	9.06	2.4	-53.8 to -70.6
60	26	1.05	13.31	4.6	-55.1 to -68.2
50	25	.91	4.86	2.5	-53.7 to -63.9
40	24	.52	3.76	1.5	-51.3 to -62.6
20	11	.71	4.44	1.9	-44.4 to -57.7

Table 18 b.

VIZB Relative Humidity Sensor Functional Precision Statistics at Various Pressure Levels

Pressure (mb)	Sample Size	Humidity Difference: [RMS	Kurt	Absolute Max]	Humidity Range:
1000	23	3.43	5.02	10.9	96.5 to 16.3
900	28	1.86	4.17	5.4	96.1 to 15.5
850	32	1.15	2.36	2.4	96.5 to 13.5
700	33	2.72	13.57	12.5	95.7 to 13.5
600	33	2.38	5.70	7.0	94.9 to 13.0
500	33	2.53	4.54	7.3	93.9 to 7.7
400	32	2.66	3.69	7.1	85.7 to 12.1
300	31	2.23	4.66	6.5	61.8 to 12.3

Table 18 c.

VIZB Height Calculation Functional Precision Statistics at Various Pressure Levels

Pressure (mb)	Sample Size	Height Difference: [RMS	Kurt	Absolute Max]	Height Range:
1000	23	0.40	2.39	0.8	240 to 91
900	28	1.09	14.90	5.0	1091 to 931
850	32	1.88	19.66	9.5	1588 to 1410
700	33	3.45	20.12	17.7	3222 to 2920
600	33	5.24	17.35	25.8	4478 to 4075
500	33	6.84	16.18	33.0	5929 to 5389
400	32	6.12	2.65	14.2	7641 to 6923
300	32	9.54	2.92	25.4	9740 to 8855
250	31	12.36	3.29	35.2	11010 to 10082
200	30	15.77	4.02	49.5	12467 to 11561
150	29	18.01	4.05	55.8	14270 to 13462
100	29	21.28	3.76	63.9	16723 to 16087
80	28	22.84	2.93	59.9	18103 to 17503
60	26	24.17	2.65	53.7	19890 to 19304
50	25	23.06	2.63	51.9	21048 to 20449
40	24	25.35	2.51	51.3	22484 to 21845
20	11	29.57	2.31	54.7	26998 to 26251

6. SUMMARY/CONCLUSIONS

The following summary and conclusions were drawn from this set of functional precision tests:

The functional precision of VIZ Model 1492-520 (VIZB) radiosonde was determined using the National Weather Service functional analysis test package. The comparisons were made from 33 flights of paired radiosondes suspended from the same balloon. Results are summarized for simultaneous measurements at one minute intervals as well as measurements at a predefined set of pressure levels. These tests were conducted for the acceptance of contract production samples and results are reported for use by the meteorological community in specifying the characteristics of this radiosonde, which operational use started in 1989.

For comparisons made at one minute intervals, the overall functional precision for temperature was 0.3°C and ranged from 0.3°C to 0.4°C. The precision for pressure ranged from 1.6 mb to 2.6 mb in the troposphere below 100 mb, and 1.1 mb to 1.8 mb in the stratosphere, with an overall value of 2.0 mb. Relative humidity precision was less than 2 percent.

For comparisons made at the predefined pressure levels, the functional precision for height ranged from about 2 meters near 850 mb to 21 meters near 100 mb. The functional precision for temperature ranged from 0.4°C to 0.6°C in the troposphere to 0.5°C to 1.0°C in the stratosphere. Relative humidity precisions were less than 3 percent.

Compared to the VIZA (Model 1492-510) time-commutated sonde, precisions for data sampled at the same time for relative humidity and dew-point were better (smaller RMSD) remained about the same for temperature, and became worse (larger RMSD) for pressure. Both tests used the same automated data recording and reduction methods. Differences are mainly attributed to the radiosonde design modifications and sensor placement.

The utility of the functional analysis test package (FATP), a new micro-computer based integrated system for graphical and statistical analyses of dual radiosonde data, was demonstrated.

7. REFERENCES

Ahnert, P.R., 1991: Precision and Comparability of National Weather Service Upper-Air Measurements. Proceedings Seventh AMS Symposium on Meteorological Observations and Instrumentation. January 14-18, 1991 New Orleans, LA. pp 221-226. American Meteorological Society, Boston,MA.

Hoehne, W.E., 1971: Standardized Functional Tests. NOAA Technical Memorandum NWS T&EL-12, Systems Development Office, Test & Evaluation Laboratory, Sterling, VA.

Hoehne, W.E., 1980: Precision of National Weather Service Upper-Air Measurements. NOAA Technical Memorandum NWS T&ED-16, Office of Systems Development, Test & Evaluation Division, Sterling, VA.

NWS, 1981: Federal Meteorological Handbook No. 3 - Radiosonde Observations. Second Edition, National Weather Service, Washington, D.C.

NWS, 1991: Functional Precision of National Weather Service Upper-Air Measurements Using the VIZ Manufacturing Co. "A" Radiosonde (Model 1492-510). NOAA Technical Report NWS 44, Office of Systems Operations, Engineering Division, Test and Evaluation Branch, Sterling, VA.

Schmidlin, F.J., J.K. Luers and P.D. Huffman, 1986: Preliminary Estimates of Radiosonde Thermistor Errors. NASA Technical Paper 2637.

Systex, Inc., 1990: MICRO-ART Software Technical Documentation Addendum for VIZ Radiosondes. Prepared by Systex, Inc. Beltsville, MD for the NWS.

APPENDIX

Referenced Flight Plots

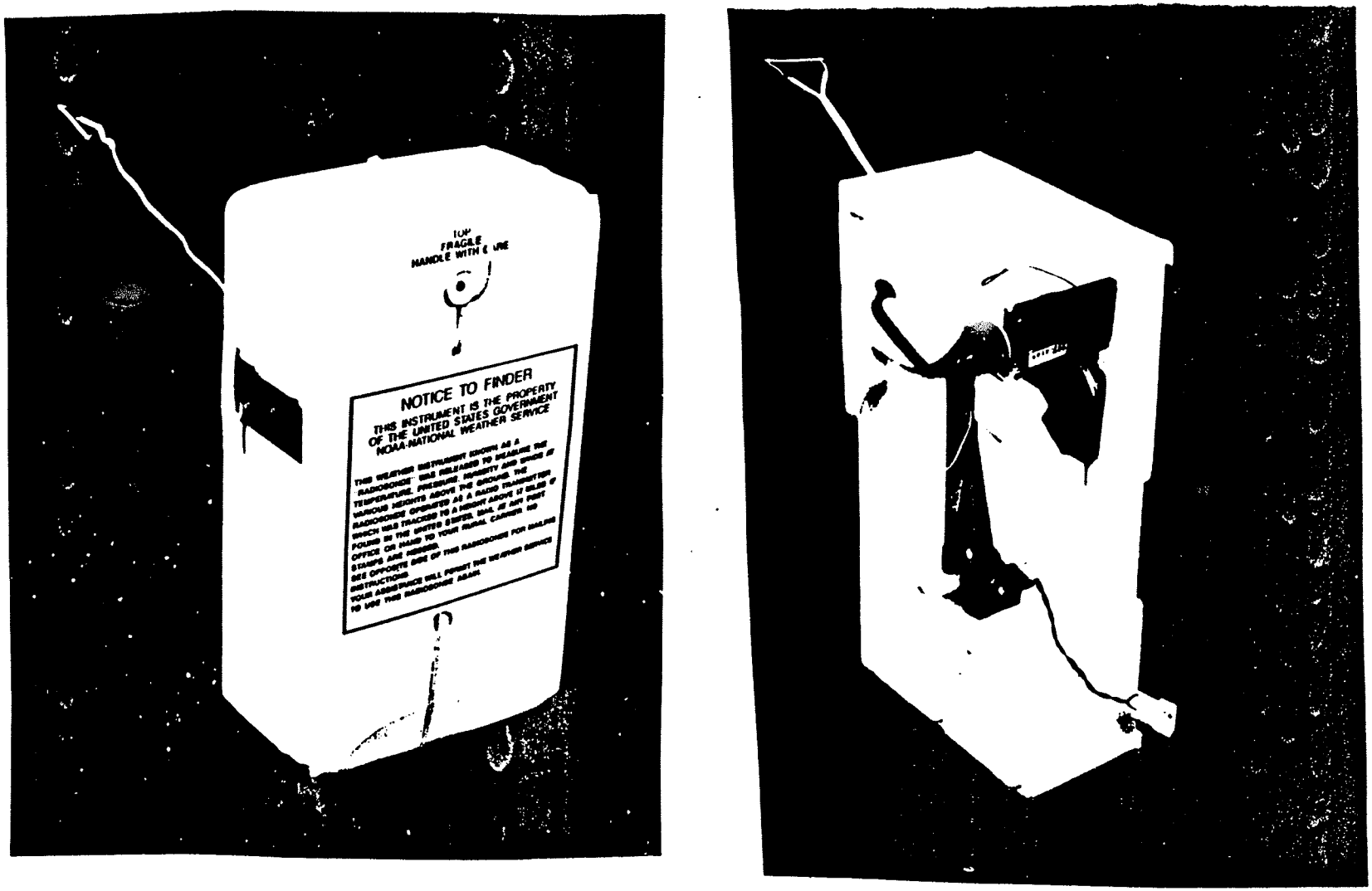

Figure A1. Illustrations of the VIZ Manufacturing Co. "B" Radiosonde (Model 1492-520).

PRESSURE DIFFERENCE VERSUS TIME
VIZB / VIZB FLIGHT # 169 11/15/88 (14:04 EST)

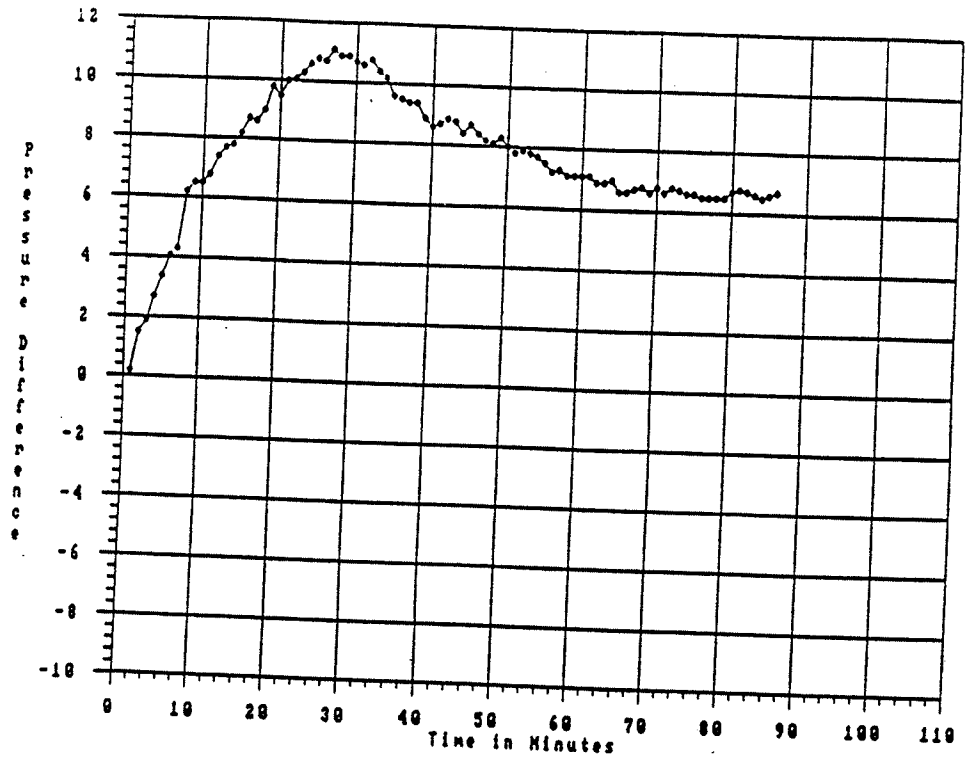

TEMPERATURE & HUMIDITY VERSUS TIME
VIZB / VIZB FLIGHT # 15 06/01/88 (12:29 EST)

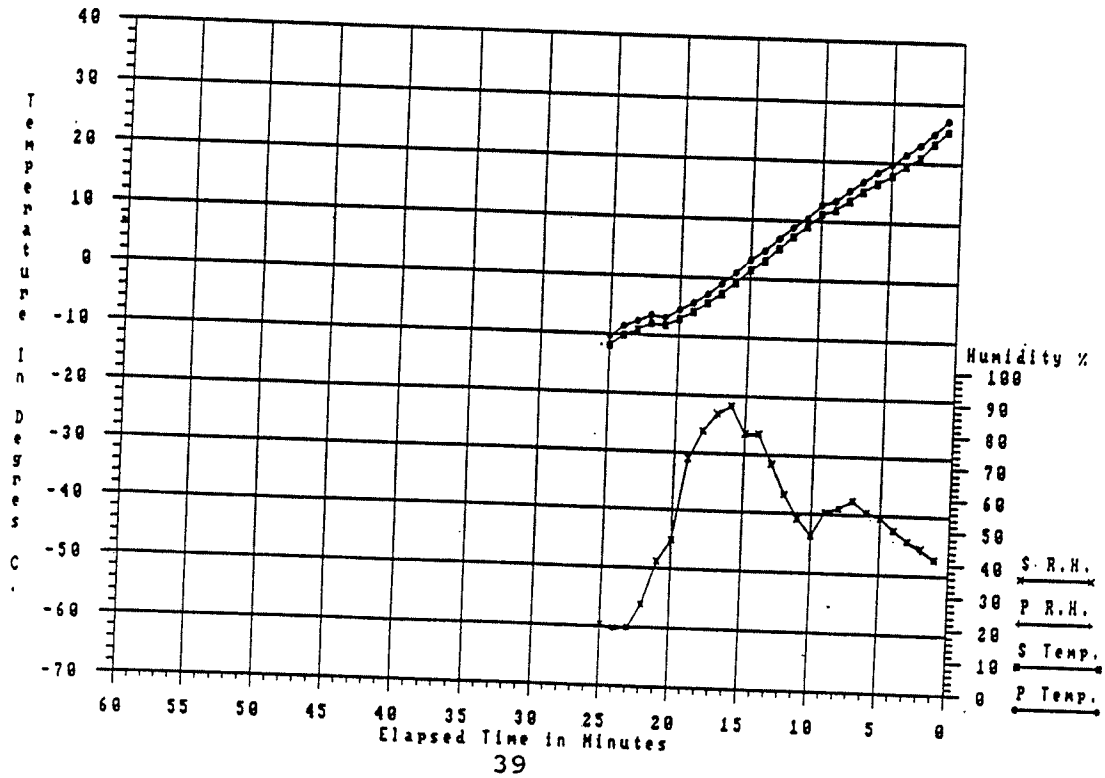

(Continued from inside front cover)

NWS 18 Joint Probability Method of Tide Frequency Analysis Applied to Apalachicola Bay and St. George Sound, Florida. Francis P. Ho and Vance A. Myers, November 1975, 43 p. (PB-251123)

NWS 19 A Point Energy and Mass Balance Model of a Snow Cover. Eric Anderson, February 1976, 150 p. (PB-254651

NWS 20 Precipitable Water Over the United States, Volume I: Monthly Means. George A. Lott, November 1976, 173 p. (PB-264219)

NWS 20 Precipitable Water Over the United States, Volume II: Semimonthly Maxima. Francis P. Ho and John T. Riedel, July 1979, 359 p. (PB-300870)

NWS 21 Interduration Precipitation Relations for Storms - Southeast States. Ralph H. Frederick, March 1979, 66 p. (PB-297192)

NWS 22 The Nested Grid Model. Norman A. Phillips, April 1979, 89 p. (PB-299046)

NWS 23 Meteorological Criteria for Standard Project Hurricane and Probable Maximum Hurricane and Probable Maximum Hurricane Windfields, Gulf and East Coasts of the United States. Richard W. Schwerdt, Francis P. Ho, and Roger R. Watkins, September 1979, 348 p. (PB-80 117997)

NWS 24 A Methodology for Point-to-Area Rainfall Frequency Ratios. Vance A. Myers and Raymond M. Zehr, February 1980, 180 p. (PB80 180102)

NWS 25 Comparison of Generalized Estimates of Probable Maximum Precipitation With Greatest Observed Rainfalls. John T. Riedel and Louis C. Schreiner, March 1980, 75 p. (PB80 191463)

NWS 26 Frequency and Motion of Atlantic Tropical Cyclones. Charles J. Neumann and Michael J. Pryslak, March 1981, 64 p. (PB81 247256)

NWS 27 Interduration Precipitation Relations for Storms-- Western United States. Ralph H. Frederick, John F. Miller, Francis P. Richards, and Richard W. Schwerdt, September 1981, 158 p. (PB82 230517)

NWS 28 GEM: A Statistical Weather Forecasting Procedure. Robert G. Miller, November 1981, 103 p.

NWS 29 Analysis of Elements of the Marine Environment for the Atlantic Remote Sensing Land Ocean Experiment (ARSLOE) -- An Atlas for October 22 through October 27, 1980. Lawrence D. Burroughs, May 1982, 116 p. (PB82 251281)

NWS 30 The NMC Spectral Model. Joseph G. Sela, May 1982, 38 p. (PB83 115 113)

NWS 31 A Monthly Averaged Climatology of Sea Surface Temperature. Richard W. Reynolds, June 1982, 37 p. (PB83 115469)

NWS 32 Pertinent Meteorological and Hurricane Tide Data for Hurricane Carla. Francis P. Ho and John F. Miller, August 1982. 111 p. (PB83 118240)

NWS 33 Evaporation Atlas for the Contiguous 48 United States. Richard K. Farnsworth, Edwin S. Thompson, and Eugene L. Peck, June 1982. 26 p.

NWS 34 Mean Monthly, Seasonal, and Annual Pan Evaporation for the United States. Richard K. Farnsworth and Edwin S. Thompson, December 1982, 85 p. (PB83 161729)

NWS 35 Pertinent Meteorological Data for Hurricane Allen of 1980. Francis P. Ho and John F. Miller, September 1983, 73 p. (PB 272 112)

NWS 36 Water Available for Runoff for 1 to 15 Days Duration and Return Periods of 2 to 100 Years for Selected Agricultural Regions in the Northwest United States. Frank P. Richards, John F. Miller, Edward A. Zurndorfer, and Norma S. Foat, April 1983, 59 p. (PB84 120591)

NWS 37 The National Weather Service Hurricane Probability Program. Robert C. Sheets, April 1984, 70 p. (PB84 182757)

NWS 38 Hurricane Climatology for the Atlantic and Gulf Coasts of the United States. Francis P. Ho, James C. Su, Karen L. Hanevich, Rebecca J. Smith, and Frank P. Richards, April 1987, 195 p.

NWS 39 Monthly Relative Frequencies of Precipitation for the United States for 6-, 12-, and 24-H Periods. John S. Jensenius, Jr., and Mary C. Erickson, September 1987, 262 p.

NWS 40 An Eight-Year Climatology of Meteorological and SBUV Ozone Data. Ronald M Nagatani, Alvin J. Miller, Keith W. Johnson, and Melvyn E. Gelman. March 1988, 123 pp.

(Continued on reverse page)